

A THESIS SUBMITTED FOR THE
DEGREE OF MASTER OF ENGINEERING

CHARACTERIZING THE ROLE
OF TRANSIENT RECEPTOR POTENTIAL
POLYCYSTIC THREE
IN ADIPOCYTE DIFFERENTIATION

AUTHOR
MATHILDE KOCH
(*B. Eng., Ecole Polytechnique*)

SUPERVISOR
PROF. MICHAEL RAGHUNATH

MAY 16TH, 2016

DEPARTMENT OF BIOMEDICAL ENGINEERING
FACULTY OF ENGINEERING
NATIONAL UNIVERSITY OF SINGAPORE

Declaration

I hereby declare that this thesis is my original work and it has been written by me in its entirety. I have duly acknowledged all the sources of information which have been used in the thesis.

This thesis has also not been submitted for any degree in any university previously.

Mathilde Koch

Mai 16th, 2016

Acknowledgments

I would like to thank Professor Michael Raghunath for his excellent guidance on this project, his availability to discuss the various challenges I faced and the quality of his insight. Enhancing my critical and scientific mind under his knowledgeable supervision has been a great pleasure.

I also want to express my deepest gratitude to Anna Goralczyk, for her patience, her advice and all she has taught me throughout the project. It was a pleasure learning from her and working with her.

Closing this chapter of my life without mentioning Aneesa Iskander and Dinesh Parate would not be possible, as we supported each other through good and bad times. Thank you for being there with me on all occasions.

Finally, I want to address my thanks to all group members for their warm welcome and support throughout my project.

Contents

Acknowledgments	ii
Table of Contents	iv
Abstract	v
List of Tables	vii
List of Figures	ix
List of Symbols	xi
Introduction	1
0.1 Why do we need to study brown fat?	1
0.2 The Transient Receptor Potential channels family	7
0.3 Characterization of TRPP3	12
1 Materials and Methods	13
1.1 Cell culture	13
1.2 Biochemistry on the RNA level	18
1.3 Biochemistry on the protein level	20
1.4 Immunostaining	26
2 Investigating the presence of TRPP3	29
2.1 Cellular characteristics of MSC and SVF	29
2.2 Characterization on SVF-derived cells	33
2.3 Characterization on MSC-derived cells	39
2.4 Conclusions	42
3 Localization study	45
3.1 Expected localization	45
3.2 Results of this localization study	47
3.3 Conclusions	53
4 TRPP3 silencing study	56
4.1 Principle of silencing	56
4.2 Optimization	59
4.3 Results in SVF	61
4.4 Results in MSC	68

5	Discussion	71
5.1	On the importance of understanding adipocyte differentiation . .	71
5.2	Identification of TRPP3 as a target of interest	72
5.3	Localization of TRPP3	73
5.4	Characterizing the role of TRPP3	74
5.5	Pathways	75
5.6	Limitation of my study	77
	Conclusion and outlook	78
6	Appendix	81
	Bibliography	89

Summary

Obesity is a global epidemic that has not been tackled through traditional prevention techniques, and which deserves attention as it is bound to be one of the biggest strain on countries' health budgets in the 21st century, alongside age-related diseases. This is why novel strategies to treat obesity are currently explored, a most promising one being cell therapy. Due to the recent discovery of brown fat cells, which burn energy through uncoupling of the mitochondrial proton gradient, as opposed to white adipocytes that store energy, extensive work has been carried out to find triggers to brown fat differentiation or white to brown adipocyte conversion.

In this study, I characterized a member of the Transient Receptor Potential (TRP) family, Transient Receptor Potential Polycystic 3 (TRPP3), which has not previously been studied in adipocytes. After having proven that it has a different distribution expression on brown and white adipocytes, we sought to further understand its role, studying it in two different types of stem cells (Stromal vascular fraction (SVF) and mesenchymal stem cells (MSC)). We then did a localization study to see if its emplacement in the cell could help us understand its role better. We sought to co-localize it with the primary cilium, which turned out to be inconclusive and we decided to explore other strategies.

We then optimized a silencing protocol to test the effect of silencing TRPP3

on the function and differentiation of cells. We show that reducing TRPP3 expression by the small interfering RNA technique induces a decrease in UCP1 expression, which is characteristic of brown adipocytes. We also observe a decrease in mitochondrial uncoupled respiration, which prove that TRPP3 is necessary for cells to show a brown phenotype.

These results therefore show that TRPP3 is necessary for brown fat differentiation. We have therefore identified a novel receptor that could be a promising target for cell therapy against obesity.

List of Tables

1.1	qPCR thermal cycle	19
2.1	MSC markers	30
2.2	SVF markers	32
2.3	Differences and similarities in cellular characteristics between SVF and MSC	33
2.4	Differences and similarities in TRPP3 expression between SVF and MSC	43
3.1	Mander's automated analysis	52
6.1	Primers used in the study	81

List of Figures

1	Energy dissipation as heat by Uncoupling Protein 1 (UCP1) . . .	4
2	Activation of thermogenesis in brown adipocytes	6
3	Positioning of TRP in cells	8
4	Members of the TRP channel family reported to have a role in adipogenesis	9
5	Ct values for identified TRPs in trilineage differentiation	11
1.1	Time line	16
1.2	Size control of the Western blot	24
1.3	Alizarine Red staining	25
1.4	Measuring the mitochondrial respiration	25
1.5	Primary cilia staining	27
2.1	MSC in culture	31
2.2	SVF in culture	31
2.3	Gene expression of TRPP3 in SVF-derived trilineage differentiated cells	34
2.4	Gene expression of TRPP3 in SVF-derived adipocytes	35
2.5	Protein expression of TRPP3 in SVF-derived adipocytes	37
2.6	Protein expression of TRPP3 in SVF-derived adipocytes (fold changes)	38
2.7	Time evolution of the appearance of TRPP3 mRNA in SVF-derived cells	38
2.8	Protein expression of TRPP3 in MSC-derived adipocytes	41
2.9	Protein expression of TRPP3 in MSC-derived adipocytes (fold changes)	42
3.1	Staining for TRPP3 of a ciliated cell	47
3.2	Localization study at the end of differentiation	49
3.3	Manders' overlap coefficient	52
3.4	Different staining patterns were presented	54
4.1	Lipofectamine transfection principle	57
4.2	TRPP3 sequence with SiRNA cutting sites and primers used	58
4.3	Silencing optimization study	60
4.4	Differentiation control of the silencing donor	62
4.5	TRPP3 and UCP1 gene expressions in silenced brown SVF	63
4.6	TRPP3 gene and protein expression in silenced brown SVF	64
4.7	UCP1 and leptin expressions in silenced brown SVF	65
4.8	Effect of TRPP3 silencing in SVF	66
4.9	Cell metabolic activity assessment in silenced SVF-derived brown adipocytes	67

4.10 Effect of TRPP3 silencing on UCP1 expression in MSC	69
--------------------------------------------------------------------	----

Acronyms

H₂O double-distilled water.

AMP Adenosine monophosphate.

ATF-2 activating transcription factor 2.

ATP adenosine triphosphate.

BAT brown adipose tissue.

BBS Bardet-Biedl syndrome.

BMI Body mass index.

BMP7 Bone Morphogenetic Protein 7.

BSA Bovine Serum Albumin.

C/EBPs CCAT/enhancer binding protein.

cAMP cyclic adenosine monophosphate.

cDNA complementary DNA.

DAPI 4',6-diamidino-2-phenylindole.

DMEM Dulbecco's Modified Eagle's Medium.

DMSO dimethyl sulfoxide.

dsDNA double-stranded DNA.

EDTA Ethylenediaminetetraacetic acid.

FBS Fetal Bovine Serum.

FCCP carbonyl cyanide-4 (trifluoromethoxy) phenylhydrazone.

HBSS Hank's Balanced Salt Solution.

HCl Hydrochloric acid.

HG High Glucose.

HRP horseradish peroxidase.

IBMX 3-isobutyl-1-methylxanthine.

Kif3a Kinesin Family Member 3A.

LG Low Glucose.

mRNA messenger RNA.

MSC mesenchymal stem cells.

NaCl Sodium chloride.

OCR oxygen consumption rate.

p38MAPK p38 mitogen-activated protein kinase.

PAGE Polyacrylamide Gel.

PBS phosphate buffered saline.

PCR Polymerase Chain Reaction.

PET positron-emission tomography.

PFA paraformaldehyde.

PGC-1 α PPAR γ co-activator α .

PKA protein kinase A.

PKD Polycystic Kidney Disease.

PKD1 Polycystic Kidney Disease 1.

PKD2L1 Polycystic Kidney Disease 2-Like 1.

PPAR γ peroxisome proliferator activated receptor γ .

PRDM16 PR domain containing 16.

qPCR Quantitative Polymerase Chain Reaction.

RACK1 receptor for activated C kinase 1.

Ripa Radioimmunoprecipitation assay.

RNA Ribonucleic acid.

SDS Sodium dodecyl sulfate.

SiRNA Small interfering RNA.

SNS sympathetic nervous system.

SVF Stromal vascular fraction.

T3 triiodothyronine.

TBP TATA-binding protein.

TBS Tris Buffered saline.

TBST Tris Buffered saline with 0.1 % Tween20.

TML tissue modulation lab.

Tris Tris(hydroxymethyl)aminomethane.

TRP Transient Receptor Potential.

TRPM8 Transient Receptor Potential Melastatin 8.	UCP1 Uncoupling Protein 1.
TRPP3 Transient Receptor Potential Polycystic 3.	WB Western Blot. WHO World Health Organisation.

Introduction

0.1 Why do we need to study brown fat?

0.1.1 Obesity is on the rise

The definition of obesity, given by the World Health Organisation (WHO), is having a Body mass index (BMI) above a 30. It has long been considered a developed countries' problem. However, the prevalence of obesity has increased worldwide, and is bound to continue on this trend as Western life-style and consumption habits are adopted by larger swathes of global population (James (2004)). While obesity in itself is not a disease, it leads to increased risks of developing various conditions. Due to higher prevalence of diabetes in Asians compared to Caucasians at equivalent BMI, the BMI threshold has been adjusted downwards in those populations to define obesity (Ntuk et al. (2014)).

0.1.2 The health-related problems caused by obesity

Two of the most important issues for which obesity is an aggravating factor are cardiovascular diseases and diabetes, which both cause millions of deaths each year around the world (WHO (2012)). They make obesity a worrying public health issue, that has been qualified as a global epidemic. Finding ways to cure obesity-related metabolic diseases, or reduce the prevalence of obesity, is therefore one of the most pressing issues facing 21st century governments and

health-care firms, along with aging-related disorders.

0.1.3 Current treatments against obesity

While some governments have focused on prevention and health care education, as obesity is a mostly preventable condition, this has not seemed to stem the epidemic, and increasing public funding is dedicated to fighting obesity through other means. While some treatments aim to diminish the sensation of hunger or increase the feeling of satiety, these have side effects that complicate further patients' lives. And the current treatments of diabetes require a quasi-permanent control of the patient's insulin and sugar levels, which cause diabetes to be a disabling condition. They allow the patient to live a normal life, but with no hope of ever being free of the disease, as they treat the symptoms but not the cause.

0.1.4 Novel therapies

Due to the importance of the issue at hand and the current lack of satisfying treatment options for obesity and its related metabolic diseases, consequent funding has been dedicated in the past years to finding a cure through bioengineering techniques. An important part of these novel therapies are cell-based: they aim to use the patient's own cells to fight his or her disease. These methods have the advantage of being tailor-made for a patient, and to cure the disease instead of merely treating the symptoms. A natural target for those therapies are adipocytes, the fat and energy-storing cells of the body.

0.1.5 The functions of adipose tissue

Obesity is caused by an imbalance between energy expenditure and energy intake. Evolutionarily, adipose tissue, composed of adipocytes, was used to store excess energy as triglycerides (Kershaw and Flier (2004)), acting as a buffer energy store which could be used in times of food shortage. Adipose tissue also provided heat isolation, and it is now known to be an important paracrine and endocrine organ (Siiteri (1987)). Therefore, when energy intake exceeds energy expenditure, as can be the case in humans enjoying food security and a sedentary lifestyle, the fat tissue functions as it was evolved to do and stores this extra energy. A continuous storing of this extra energy eventually turns into weight gain and obesity if the patient's habits remain unchanged. The cells storing this energy excess are called white fat cells, or white adipocytes, as opposed to brown adipocytes described thereafter.

0.1.6 The recent discovery of brown fat in human adults

It was thought until 2009 that only hibernating rodents or human babies possessed another type of fat, called brown fat or brown adipocyte, which burns lipids when properly stimulated, in a process termed "non-shivering thermogenesis". This was evolved to maintain the hibernating animals' temperature, or the baby's temperature before its muscles fully develop. However, in 2009, brown fat was discovered in humans through positron-emission tomography (PET) scans, as highly metabolically active zones in the body after cold exposure (Virtanen et al. (2009)). Those cells have the potential to dissipate the body's energy excess instead of storing it. The therapeutic potential of brown fat led to increased research on its mechanisms and activation strategies.

0.1.7 UCP1: its role in brown fat

UCP1 is a protein found on the mitochondrial membrane, that uses the proton gradient of the electron transport chain to dissipate energy and produce heat instead of adenosine triphosphate (ATP) (see Figure 1). It has become a hallmark of brown adipose tissue (BAT) (Aquila et al. (1985), Cannon and Nedergaard (2004)).

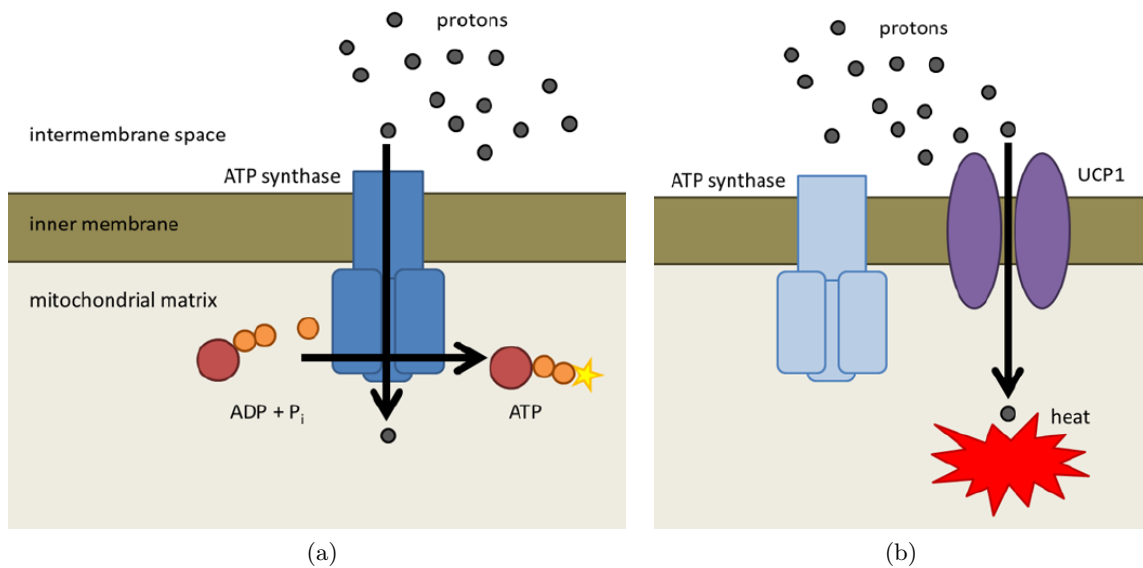


Figure 1: **Energy dissipation as heat by UCP1**

(a) The proton gradient over the inner mitochondrial membrane facilitates ATP production by ATP synthetase. (b) UCP1 uncouples the proton gradient from ATP synthesis, dissipating energy as heat.

Figures reproduced with permission from Anna Goralczyk

0.1.8 Origins of increased thermogenesis

There are three different pathways to obtain increased thermogenesis of adipose tissue that need to be understood:

1. *Stimulation*: the stimulation of already-expressing UCP1 brown adipocytes, which then exhibit more important uncoupled respiration and thermogenesis.

2. *Conversion*: the conversion of white adipocytes into brown adipocytes.

Those two cells types come from different developmental origins but some white cells, deemed "beige", can be converted to a brown phenotype despite their different histories. The gain of UCP1 by those cells is also called *browning*.

3. *Differentiation*: the differentiation of progenitor cells residing within the adipose tissue into brown adipocytes. This process is also called *recruitment*

Those three processes need to be differentiated when interpreting experimental results, and particularly increased UCP1 expression.

0.1.9 Adrenergic activation of brown fat

The first step to unlock brown adipocytes' therapeutic potential is to understand how they develop and their usual pathways of activation.

Two main transcription factors regulate both white and brown adipocyte differentiation: peroxisome proliferator activated receptor γ (PPAR γ) and CCAT/enhancer binding protein (C/EBPs) (Schulz and Tseng (2013), Wu et al. (1999)). More specifically, both nuclear PPAR γ co-activator α (PGC-1 α) and the transcription factor PR domain containing 16 (PRDM16), known to interact with C/EBPs (Kajimura et al. (2009), Schulz and Tseng (2013)), control the brown adipocyte differentiation program.

Once differentiated, cold temperatures stimulation activates brown adipocytes through the sympathetic nervous system (SNS). Norepinephrine released from sympathetic neurons activates β -adrenergic and cAMP-dependent pathways (Bonet et al. (2013)). PKA is activated by increased intracellular levels of cAMP, and

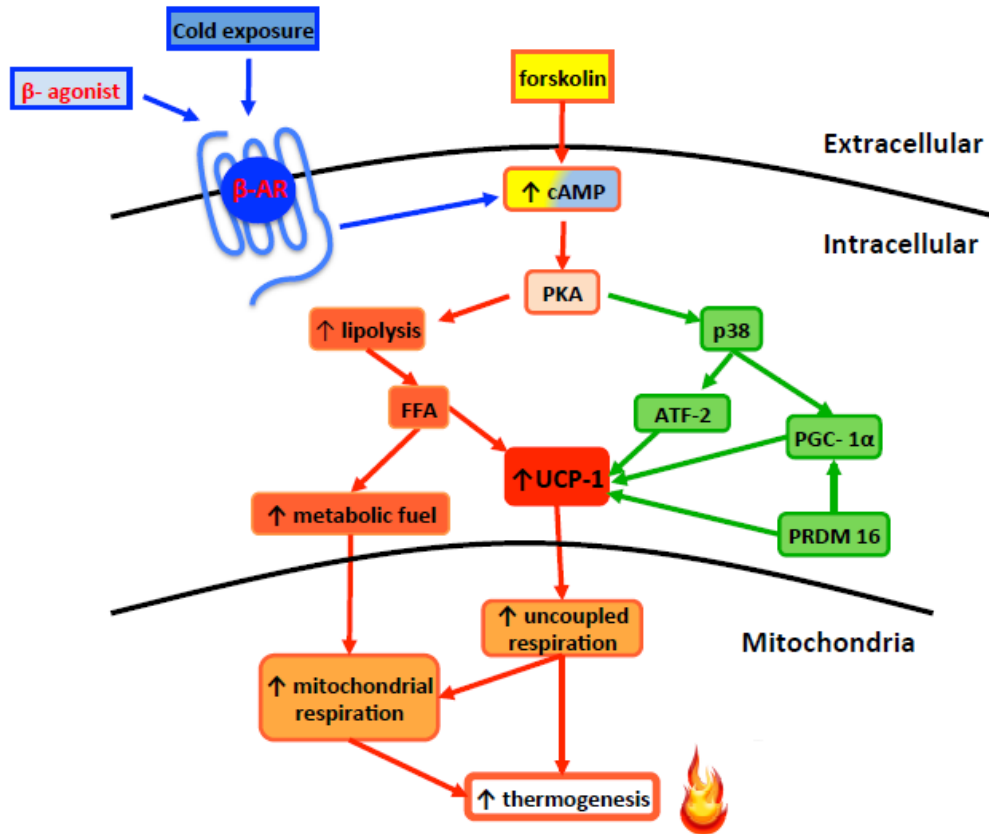


Figure 2: **Activation of thermogenesis in brown adipocytes via the β -adrenergic pathway:** β -adrenergic pathway stimulation through cold exposure or pharmaceutical reagents leads to increased level of cyclic adenosine monophosphate (cAMP) (Gannier et al. (1994)). This augments levels of protein kinase A (PKA), which in turn initiates a signalling pathway that results in a surge in the metabolic capacity of the cell, UCP1 transcription and thermogenesis. *Figures reproduced with permission from Michelle Lee.*

then phosphorylates p38 mitogen-activated protein kinase (p38MAPK). Phosphorylated p38MAPK can drive UCP1 expression in a dual manner: it either phosphorylates activating transcription factor 2 (ATF-2) (Lee et al. (2016)) or activates PGC-1 α (Bonet et al. (2013)) (see Figure 2). This is why it is known as a key player in brown adipocyte response to sympathetic stimulation (Cao et al. (2004)).

Other reports have described activators of the thermogenic program in brown adipocytes: β -adrenergic agonists (like isoproterenol) and cAMP inducers (like forskolin) (Seale et al. (2008), Wang et al. (2008)).

0.1.10 Need for non-adrenergic activation strategies

However, using the adrenergic pathway previously described is not neutral for the patient, with possible implication of the SNS in heart failure if systematically activated (Triposkiadis et al. (2009)) . Therefore, numerous studies have looked into other ways to activate brown fat. It has been proven in mice that activation of the cold receptor Transient Receptor Potential Melastatin 8 (TRPM8) triggers UCP1-dependent thermogenesis (Ma et al. (2012)). Following these findings, it was shown in humans that stimulation of TRPM8 can induce browning of white adipocytes, ie: up-regulation of UCP1 in white adipocytes that did not go through the same lineage differentiation as brown fat cells (Rossato et al. (2014)). This raises hopes for non-adrenergic activation of brown fat through TRP channels.

0.2 The Transient Receptor Potential channels family

0.2.1 Structural commonalities of TRP channels

The TRP channels are a family of receptors, defined through sequence homology. They are poly-modal, having been shown to answer to various stimuli such as pH, temperature, mechanical forces, voltage or chemical signals. They ultimately transform those various signals into biochemical signals that can be interpreted by the cell (Hilton et al. (2015)). They have first been discovered in *Drosophila*, but since have been identified across almost all species. The 27 members of the human family have been classified in 6 sub-families: canonical (TRPC), melastatin (TRPM), vanilloid (TRPV), ankyrin (TRPA), mucolipin (TRPML) and polycystin (TRPP) (Bishnoi et al. (2013)). Sequence analysis that all TRPs

comprise 6 transmembrane polypeptide subunits that can assembled as homo or hetero-dimers to form cation-permeable pores (see Figure 3 (Clapham (2003))).

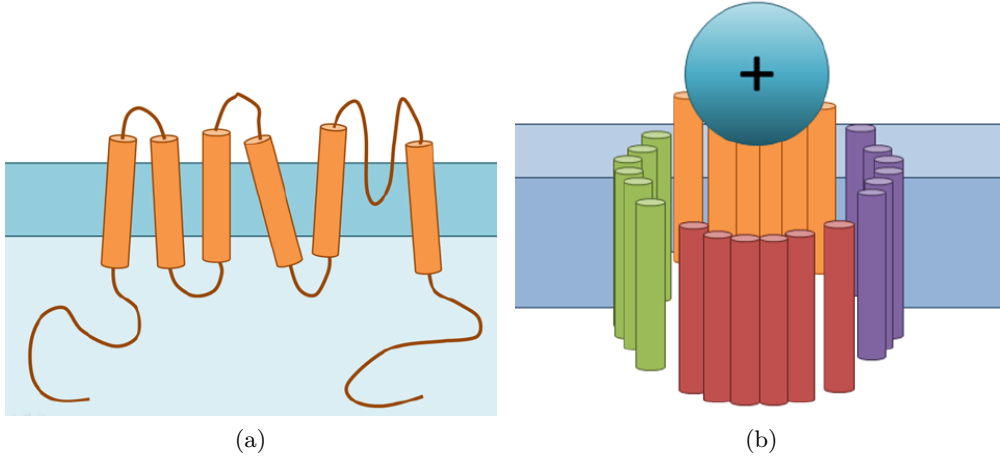


Figure 3: **Positioning of TRP in cells** (a) One TRP domain consists of 6 transmembrane domains (S1-6) with a loop between S5 and S6. Both the C and N terminal domains are intracellular. (b) 4 TRP units make one non-selective cation channel. Both homo and hetero-tetramers have been described. *Figures reproduced with permission from Anna Goralczyk*

The importance of calcium signaling in cells has been emphasized in numerous studies, and the fact that TRP channels regulate Ca^{2+} intake makes them unavoidable in understanding complex signaling processes in cells. They can generate changes in cytoplasmic Ca^{2+} concentrations either when located at the plasma membrane or at intracellular organelles that act as Ca^{2+} stores.

0.2.2 The role of TRP in adipogenesis and obesity

The current state of knowledge about the role of TRP in adipocyte function has been described (Ahern (2013)). They intervene in guts, liver, sensory pathways, taste or satiety. Based on this review, as well as on Bishnoi et al. (2013), a summary of the elucidated functions of some TRPs in adipogenesis and particularly in brown adipogenesis have been shown in Figure 4.

TRPC1 and TRPC5 have been shown by Sukumar et al. (2012), using a micro-array analysis in mice, and over-expression in human HEK immortal-

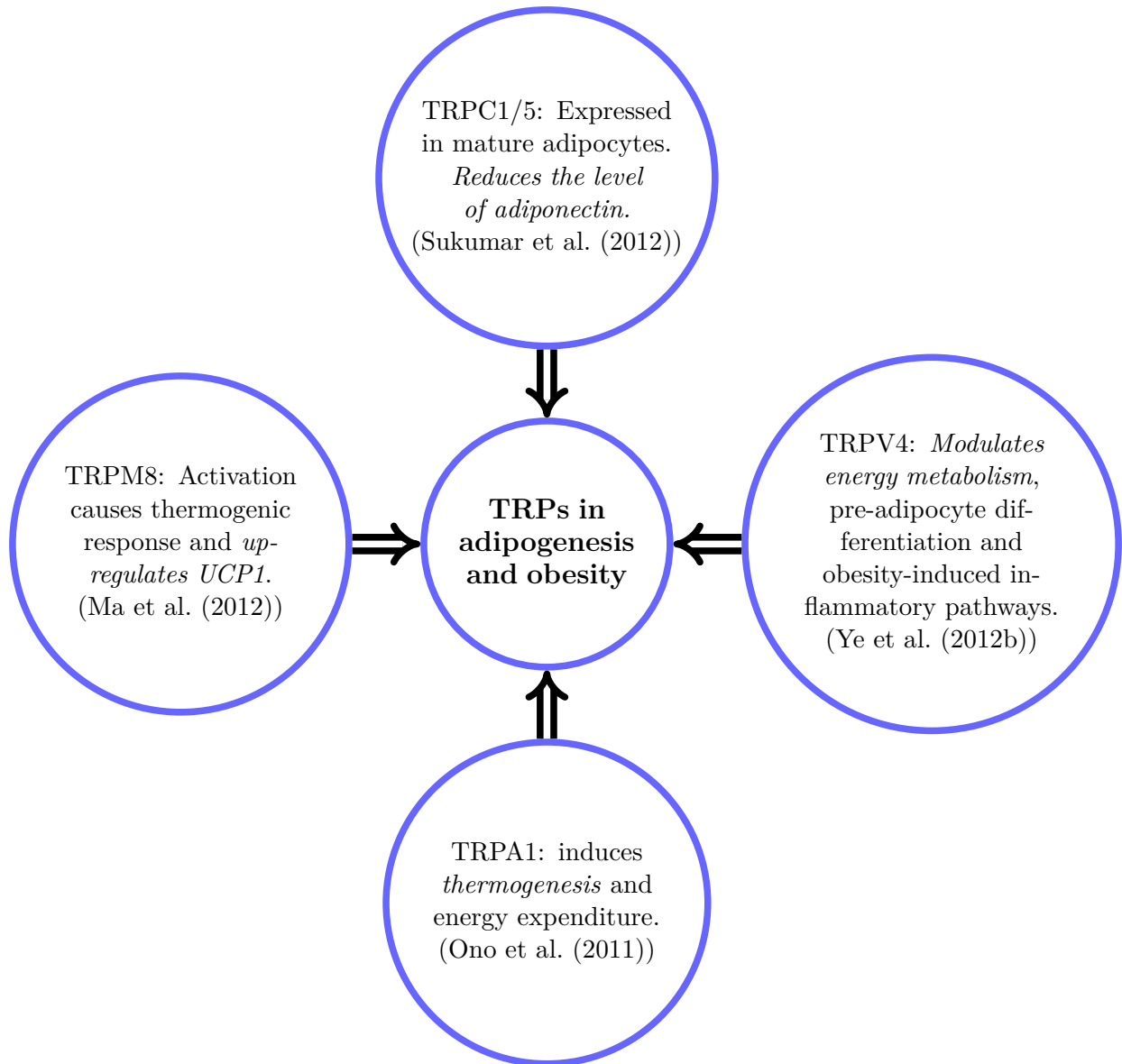


Figure 4: **Members of the TRP channel family reported to have a role in adipogenesis** Figure amended and completed from Bishnoi et al. (2013)

ized cell line, to be constitutively open in adipocytes, therefore increasing intracellular Ca^{2+} levels and inhibiting the production of insulin sensing and anti-inflammatory adipokine-adiponectin. This process is prominent in late stages of differentiation as well as in mature adipocytes (Ahern (2013)).

TRPV4 has been identified in white and brown mouse adipocytes and, according to Ye et al. (2012b), its activation reduces expression of PGC-1 α and drives expression of pro-inflammatory cytokines. According to the same group,

TRPV4-null mice exhibit greater energy expenditure, and their white adipocytes express higher levels of UCP1, suggesting that inhibiting TRPV4 might result in "browning" of white adipocytes.

Reports on the role of TRPV1 are contradictory in mice, so more research is needed to elucidate its role (Bishnoi et al. (2013)). TRPA1, when activated by capsaicin (Shintaku et al. (2012)), induces thermogenesis in rats (Ono et al. (2011)).

The role TRPM8 has already been mentioned (0.1.10). As shown in the Figure, growing evidence suggests a role for TRPs in adipocyte function and differentiation, a role that could potentially be exploited for therapeutic use.

0.2.3 The necessity of a human study

As has been shown in 0.2.2, the role of TRP channels in adipocytes and particularly in brown adipogenesis is slowly being uncovered. However, excepting TRPM8, all of those studies were conducted in animals or in immortalized human cell lines from one of them. However, there are important differences between mouse and human biology, and understanding TRP channels' roles in energy homeostasis requires studies in human cells. This is why an extensive study of TRPs in adipocyte differentiation was conducted in the tissue modulation lab (TML).

0.2.4 The study of TRP in adipogenesis

The aim of this study was to identify potential TRP channels, not mentioned in the literature, that could impact adipogenesis in general, and brown adipogenesis in particular. The chosen method was to detect up-regulation of genes through Polymerase Chain Reaction (PCR), during the lineage commitment of cells to

either brown or white fat, with or without the crowding protocol used in the lab and recently published (Lee et al. (2016)). Macromolecular crowding has been shown to favor adipogenesis through increased matrix deposition (Ang et al. (2014)), and in particular brown adipogenesis (Lee et al. (2016)).

This study was done in 3 parts. The *first aim* was to identify TRP genes that were regulated differently in MSC, brown or white adipocytes (data not shown). Once those few genes were identified, the *second part* consisted of a differentiation study, comparing the regulation of those genes in the three lines of differentiation possible for MSC: adipocytes, chondrocytes or osteoblasts (Figure 5). The aim was to differentiate between genes that were linked to loss of pluripotency by stem cells, or to their aging, and genes linked to gain of function by adipocytes.

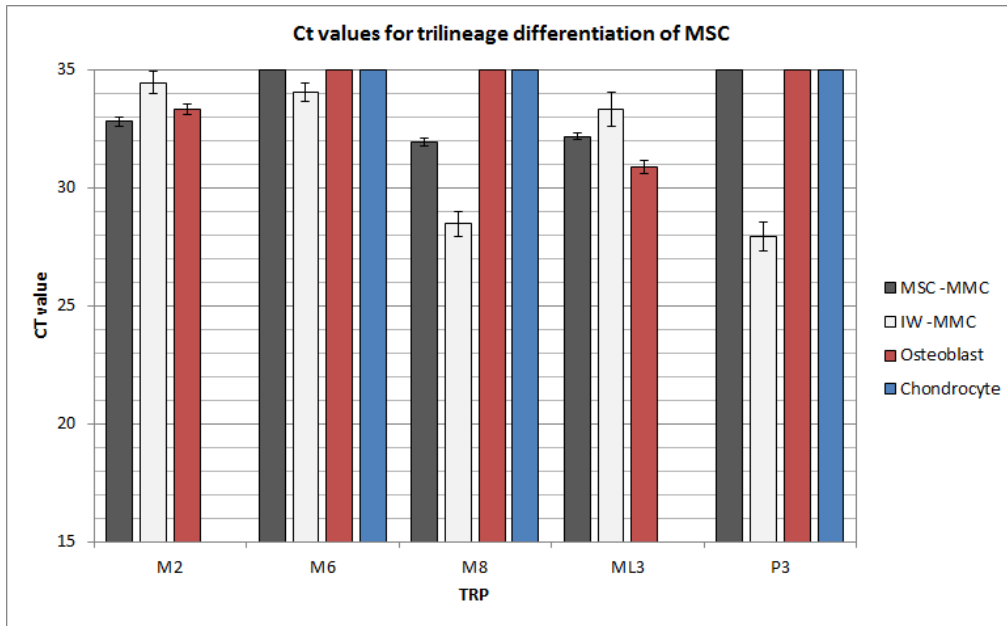


Figure 5: **Ct values for identified TRPs in trilineage differentiation**
Figure adapted from Marc Van Vijden; n=3

If the up or down-regulation of those genes was lineage specific, the *third part* of the study, a time-evolution of the occurrence of those genes, was conducted. Those studies were conducted before my arrival. As expected, TRPM8 was identified through this study.

0.3 Characterization of TRPP3

0.3.1 Identification of TRPP3 as a potential target

Due to this previously conducted studies (0.2.4), TRPP3 was identified as an interesting, and never studied in adipocyte, target for further characterization. Being a known cation-permeable channel (Chen et al. (1999)), regulated by a wide range of stimuli, ranging from pH, voltage and changes in cell volume (Shimizu et al. (2009)) to alkalization (Shimizu et al. (2011)) or temperature (Higuchi et al. (2014)), TRPP3, also known as Polycystic Kidney Disease 2-Like 1 (PKD2L1), has mostly been studied in sour tasting (Ishimaru et al. (2006)). The robustness of the preliminary data and the lack of current literature on the topic of TRPP3 involvement in adipogenesis induced us to want to characterize it further.

0.3.2 Aim of the Masters project

This project was separated in a three different parts. The *first part* of the project consisted of a full characterization of behaviors in SVF and MSC, as to assess in which cell type we were to conduct further experiments. Once the results were established on the Ribonucleic acid (RNA) level, the study was pursued to establish them on the protein level. The *second aim* was to establish the localization of TRPP3, which could give us hints as to its exact role. The *third part* consisted of a silencing study in order to assess the effect of the absence of TRPP3 on differentiation and function of the studied tissues.

The working hypothesis behind this work was that TRPP3 was a brown adipocyte marker, that was involved in the differentiation and function of brown fat.

Chapter 1

Materials and Methods

1.1 Cell culture

All the mentioned media are filtered before each media change as we are cultivating the cells without antibiotics.

1.1.1 Cells extraction

The progenitor cells, isolated from the SVF of abdominal subcutaneous adipose tissue were obtained from Dr Sue Anne Toh at passage 4.

Recruited subjects were 21 years old, obese with body mass index (BMI $\geq 35 \text{ kg} \cdot \text{m}^{-2}$), and candidates for bariatric surgery. Patients with the following conditions were excluded from this study: diabetes mellitus (defined as HbA1c >6 or fasting glucose $\geq 6.0 \text{ mmol} \cdot \text{L}^{-1}$), a history of malabsorption syndrome, Crohn's disease, ulcerative colitis, pancreatitis, or a history of ingesting drugs known to alter insulin sensitivity (e.g., corticosteroids). Informed consent was obtained from all donors, recruited from a pool of patients of the Center for obesity and metabolic surgery, National University Health System (NUHS, Singapore). Their baseline anthropometric measurements, complete medical his-

tory, blood pressure measurement, presence of other cardiovascular disease risk factors (e.g., hypertension, dyslipidemia, smoking, and alcohol intake), physical examination, presence of albuminuria, and all existing medications prescribed were collected as their detailed medical history.

The adipose tissue extracts were obtained from the subcutaneous abdominal area towards the end of the bariatric surgery, without any additional surgical procedure. Ethics approval was obtained from the National Healthcare Group Domain Specific Review Board (Singapore) and the procedures were carefully carried out in accordance with the approved guidelines.

The MSC were purchased from Lonza, extracted from young patients's bone marrows.

1.1.2 SVF and MSC culture

The following protocols are written for SVF, however, when MSC experiments were carried out, we followed the same protocols.

The cells were cultured in (Low Glucose (LG)Dulbecco's Modified Eagle's Medium (DMEM)) supplemented with GlutamaxTM (10567-04 Gibco) and 10 % Fetal Bovine Serum (FBS) at 37 °C in 5 % CO₂ in T-75 cm flasks. The media was changed every 2 d to 3 days.

They were then passaged at around 90 % confluence using a 5 min to 10 min incubation with 2.5 mL TrypLETM Express (12604, Gibco/Life Technologies), until observed detachment from the surface with a microscope. The trypsin was then inhibited by dilution in 7.5 mL of media, the mixture transferred into a 15 mL tube and spun down to form a pellet at 10 000 rpm for 5 min. During expansion, the cells were divided in 3 and seeded in T-75 cm flasks in 12 mL media. Before seeding for experiments, the cells were counted using Trypan blue

staining.

They were then seeded at passage 6 at a density of $10\,000\text{ cells} \cdot \text{mL}^{-1}$ with 1 mL per well for a 12-well plate, 0.5 mL per well for a 6-well plate or a 4-well Labtek chamber and 250 μL per well for a 8-well Labtek chamber.

1.1.3 Freezing media

The freezing solution for cells designed to be kept for further experiments is made of 50 % LGDMEM, 40 % FBS and 10 % dimethyl sulfoxide (DMSO) (D2650, Sigma-Aldrich, St- Louis, MO, USA). The cells frozen with this solution were kept in liquid nitrogen tanks, and gradually cooled down with a one-day incubation at -80°C before transfer in the tanks.

1.1.4 Macromolecular crowding

The differentiation are either supplemented with crowders (+) or not (-). We use a combination of two crowders according to protocol from Dewavrin et al. (2015). We supplement the culture media with $37.5\text{ mg} \cdot \text{mL}^{-1}$ of Ficoll 70 (GE Healthcare, FicollTM PM70, lot n° 10085600) and $25\text{ mg} \cdot \text{mL}^{-1}$ of Ficoll 400 (GE Healthcare, FicollTM PM400, lot n° 10225087).

1.1.5 Osteoblast differentiation

The osteoblast differentiation media is made of High Glucose (HG)DMEM supplemented with GlutamaxTM (10569-010 Gibco), supplemented with 10 % FBS, 0.1 μM Dexamethasone (D4902, Sigma-Aldrich, St- Louis, MO, USA), 100 μM Ascorbic Acid (019-12063, Wako, Osaka, Japan) and 10 mM β -glycerophosphate (35675, Calbiochem, Merck Millipore, Darmstadt, Germany).

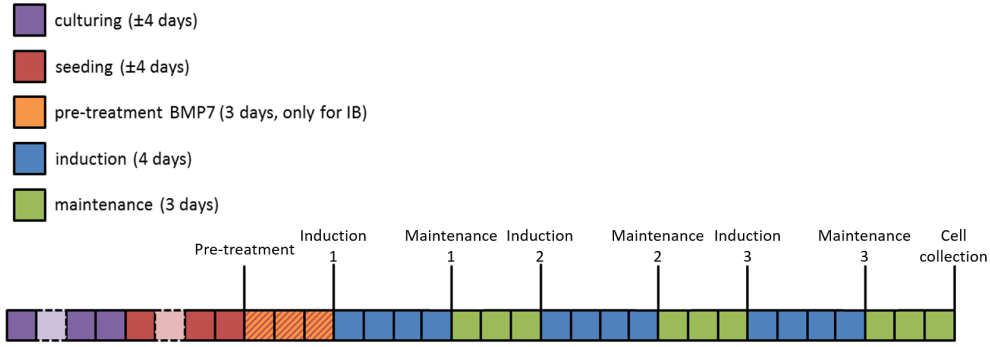


Figure 1.1: Time line of adipocyte differentiation.

1.1.6 Chondrocyte differentiation

Chondrocytes were obtained as a courtesy of Marc Rabaza Gairi who followed this protocol and checked the differentiation using Quantitative Polymerase Chain Reaction (qPCR) for chondrocyte genes. The cells are not plated but cultured in pellet culture in 15 mL polypropylene tubes.

The chondrocyte differentiation media is made of HGDMEM supplemented with GlutamaxTM (10569-010 Gibco), supplemented with 0.1 μM Dexamethasone (D4902, Sigma-Aldrich, St- Louis, MO, USA), 1 % ITS + Premix, 50 $\mu\text{g} \cdot \text{mL}^{-1}$ Ascorbic Acid (019-12063, Wako, Osaka, Japan), 1 % MEM Sodium Pyruvate (Gibco), 4 mM Proline, 1 % Pen/Strep (Gibco), 1 % L-Glutamine (Gibco) and 10 $\text{ng} \cdot \text{mL}^{-1}$ TGF- β 1.

1.1.7 Adipocyte differentiation

The differentiation is made of different phases. First, a pre-treatment phase, and then 3 cycles of induction-maintenance each a week long, the induction lasting 4 days and the maintenance 3 (See Figure 1.1).

The pretreatment, when cells are confluent, lasts 3 days. The cells are still cultured in LGDMEM and 10 % FBS. The macromolecular crowding starts at this point for cells that will be differentiated in crowded media. For the cells

that will be differentiated in brown cells, the media is supplemented with 8 nM Bone Morphogenetic Protein 7 (BMP7) (354-BP, R & D Systems, Minneapolis, MN, USA).

The white adipocyte induction media is made of HGDMEM, supplemented with 10 % FBS, 1 μ M Dexamethasone (D4902, Sigma-Aldrich, St- Louis, MO, USA), 10 μ g \cdot mL⁻¹ Insulin (I6634, Sigma-Aldrich, St- Louis, MO, USA), 0.2 mM Indomethacin (I7378, Sigma-Aldrich, St- Louis, MO, USA) and 0.5 mM 3-isobutyl-1methylxanthine (IBMX) (I5879, Sigma-Aldrich, St- Louis, MO, USA).

The brown adipocyte induction media is made of white adipocyte differentiation media, supplemented with 1 μ M Rosiglitazone (ALX-350-125, Enzo Life Sciences Inc., Farmingdale, NY, USA) and 1 nM triiodothyronine (T3) (T5516, Sigma-Aldrich, St- Louis, MO, USA).

For both differentiation protocols, the maintenance media is HGDMEM, supplemented with 10 % FBS, and with or without macromolecular crowders in accordance with the previous steps.

1.1.8 Silencing with Small interfering RNA (SiRNA)

We used a Lipofectamine[®] 2000 (11668, Invitrogen, Carlsbad, CA, USA)-mediated SiRNA (SR305958, Origene, Rockville, MD, USA) method for silencing. We combined manufacturers' instructions to obtain the following protocol: the silencing starts 1 week after the beginning of differentiation, at the step called induction 2 in the previous time line (Figure 1.1). The following protocol is applied with each media change, and written for a 24-well plate.

First, the media is changed according to usual protocols, with the concentrations of all reagents multiplied by 6/5, as 100 μ L of silencing solution will be added to the 500 μ L of media already in the well.

Then, the silencing solution is prepared: the SiRNA (20 nM concentration, or 12 pmol in total) is diluted in 50 μ L of serum-free HG or LG media (depending on the media used in the solution it will be added to). Then, Lipofectamine[®] 2000 is diluted 1/100 in 50 μ L of serum-free HG or LG media, and incubated 5 min at room temperature. The two solutions are then mixed and incubated 20 min at room temperature. Finally, 100 μ L of the SiRNA/Lipofectamine[®] solution are added in each well.

For controls, we use the same protocol for the Universal Scrambler (SR30004, Origene, Rockville, MD, USA), which does not recognize any human sequence and therefore should not silence genes of interest. We also use the same protocol without adding SiRNA to test the effect of Lipofectamine[®] 2000 alone. We also keep a control where we just add the 100 μ L of serum-free HG or LG media when we add it in the other wells.

1.2 Biochemistry on the RNA level

1.2.1 RNA isolation

Cells grown on 24-well plates are rinsed twice with Hank's Balanced Salt Solution (HBSS) and incubated at room temperature for 5 min with Trizol[®] (15596, Gibco/Life Technologies, Carlsbad, CA). We then proceed with phenol-chloroform extraction (C2432, Sigma-Aldrich, St- Louis, MO, USA) and of RNeasy[®] Mini Kit 250 (74106, Qiagen, Hilden, Germany) according to manufacturer's instructions. The RNA is kept at -80°C until further processing, as well as the Trizol remains.

Temperature (°C)	95	94	58	72	60	94	25
Time (min:sec)	5:00	0:15	0:30	0:30	0:30	0:30	0:30
Repeats	1	35			1	1	1

Table 1.1: **qPCR thermal cycle.**

1.2.2 complementary DNA (cDNA) synthesis

Concentration of the isolated RNA was measured after thawing, just before cDNA synthesis, using Nanodrop (ND-1000, Thermo Fisher Scientific Inc., Waltham, MA, USA) to determine the absorbance ratio at 260 280 nm. The messenger RNA (mRNA) was converted to cDNA using the MaximaTM First Strand cDNA synthesis kit (K1642, Fermentas, Thermo Fisher Scientific Inc., Rockford, IL, USA) according to manufacturer's instructions.

1.2.3 qPCR

Real-time qPCR was performed using MaximaTM SYBR Green/ROX qPCR Master Mix (K0222, Fermentas, Thermo Fisher Scientific Inc, Rockford, IL, USA) in a real-time PCR machine (MxPro 3000PQPCR, Stratagene, Agilent Technologies Inc., Santa Clara, CA, USA). Primers are listed in Table 6.1. The qPCR thermal profile is shown here 1.1

The expression is normalized with TBP (TATA-Box Binding Protein) as a house-keeping gene, using the $2^{\Delta\Delta CT}$ method. T-tests were performed and results are shown as follows on the graphs: * means p-value <0.05, ** means p-value <0.01 and *** means p-value <0.001. No * means results are not significant.

1.2.4 Primers design

Primers listed in Table 6.1 have been either looked for in literature or designed using the Primer Blast tool (Ye et al. (2012a)). Those found in literature have been verified using this tool.

The design process is as follows: a first search with the accession number of the gene of interest returns the 10 best primers according to Primer Blast. Looking at the size of the final product and the sizes of the possible non-desired side products, this list is reduced to one or two primers, that have only a few side products and that are smaller than 300 bp (chosen given the sizes of known primers used by the team: it should not be longer than this).

Then, a thorough investigation of those side products is conducted: I looked at where the mismatches were, and due to which primer, the forward or the reverse. Then, when the primer that is causing the side products is identified, I looked at the sequence of the gene of interest, and launched Primer Blast searches adding 2 bases at the end of the primers: either 2 on the same side or 1 on each side. These new searches allowed me to find which design has no side products that could disturb the PCR. The designed primers are then ordered.

1.3 Biochemistry on the protein level

1.3.1 Protein collection

Proteins are collected from cells mono-layers as whole cell lysates with Radioimmunoprecipitation assay (Ripa) buffer (50 nM Tris(hydroxymethyl)aminomethane (Tris) (1400, First Base, Selangor, Malaysia), 7.8 pH, 150 nM Sodium chloride (NaCl), 0.5 % Na Deoxycholate, 1 % Triton X-100, 0.1 % Sodium dodecyl sulfate (SDS)) supplemented with 1 nM protease inhibitor cocktail (04 906 845 001,

Roche, Basel, Switzerland). Protein extracts can be stored at -80°C at that stage.

1.3.2 Protein extraction from Trizol[®]

Extraction from culture: See 1.2.1. For this protocol, we are using the Trizol[®] leftovers after RNA extraction.

Removal of cDNA phase: First, 0.3 mL of 100 % ethanol per 1 mL Trizol[®] Reagent used for the initial homogenization is added to the samples, and the solution is mixed well before incubating the samples for 2 min to 3 min at room temperature. The DNA is then pelleted by centrifugation at 2000 g for 5 min at 4°C . The phenol-ethanol supernatant is transferred to a clean tube for protein isolation.

Protein precipitation: 1.5 mL of isopropanol to the phenol-ethanol supernatant per 1 mL of Trizol[®] Reagent used for the initial homogenization is added to the samples, and the samples are incubated for 10 min at room temperature. The tubes are then centrifuged at 12,000 g for 10 min at 4°C to pellet the protein, and the supernatant is discarded.

Protein wash (3 repeats): The protein pellet is washed with 2 mL of the wash solution (0.3 M guanidine in 95 % ethanol) per 1 mL of Trizol[®] Reagent used for the initial homogenization for 20 min at room temperature. The samples are then centrifuged at 7500 g for 5 min at 4°C to pellet the protein, and the supernatant is discarded.

2 mL (per 1 mL of Trizol[®] Reagent) of 100 % ethanol is added to protein pellet after the third wash, and incubated for 20 min at room temperature. The samples are then centrifuged at 7500 g for 5 min at 4°C to pellet the protein, and the ethanol wash is discarded. The proteins are then left 5 min to 10 min to

air dry before proceeding to re-suspension.

Protein re-suspension: We added 30 μ L to 60 μ L Urea-SDS solution (4 M Urea and 0.5 % SDS in 1 M Tris-Hydrochloric acid (HCl), 8 pH) to the protein pellet. We then incubated 40 min at 52 °C to dissolve the pellet. The insoluble material is made to sediment by centrifugation at 10,000 g for 10 min at 4 °C. The obtained proteins are then transferred to a new tube for further experiments. Protein extracts can be stored at -80°C at that stage.

1.3.3 Western blot

Separation: The proteins are separated under reducing conditions using 8 % (for TRPP3) and 12 % (for UCP1) SDS-PAGE. They are then transferred onto a nitrocellulose membrane (0115, BioRad, Hercules, CA, USA).

Blocking: The membrane was blocked with 5 % Bovine Serum Albumin (BSA) Tris Buffered saline with 0.1 % Tween20 (TBST) for 1 h at room temperature. For UCP1, we use fatty-acid free BSA. TBST is made of Tris Buffered saline (TBS) with 0.1 % Tween 20 (Sinopharm Chemicals, China). The TBS buffer is composed of 61 g Tris (1400, First Base, Selangor, Malaysia) and 90 g NaCl dissolved in 1000 mL double-distilled water (H_2O) and adjusted to 7.6 pH. It is then stored at 4 °C.

Primary antibodies: The membranes are incubated overnight at 4 °C in 5 % BSA TBST with the following antibodies: rabbit anti-TRPP3 (1:1000, 102-12985, Raybiotech, Norcross, GA, USA), mouse anti-UCP1 (1:1000, mab6158, R & D Systems, Minneapolis, MN, USA) and mouse anti- α -tubulin (1:1000, T6074, Sigma-Aldrich, St-Louis, MO, USA) as a loading control.

The TRPP3 antibody has been raised against the following sequence (CTIS-STGPLQPQPKKPEDEPQETMNAVG), which only matches with TRPP3 when

a BLAST search is conducted on the unitprot website, in the UNITPROTKB database, for E-values under 100.

Secondary antibodies: After washing with TBST, the cells are incubated 1 h at room temperature in 3% BSA TBST with the following antibodies: HRP goat-anti mouse (1:3000, P0447, Dako, Glostrup, Denmark) or HRP goat-anti rabbit (1:3000, P0448, Dako, Glostrup, Denmark)

Detection: Chemiluminescence was captured with a Chemidoc MP Imaging System (Bio-Rad, Hercules, CA, USA) using SuperSignal West Pico (for TRPP3) or Femto (for UCP1) Chemiluminescent Substrate for detection of HRP (34080 and 34096, Thermo Fisher Scientific, Waltham, MA, USA).

Stripping After detection the membranes were stripped using the following protocol. The membranes are incubated 50 °C for 10 min while covered in harsh stripping buffer (20 mL SDS 10 %, 12.5 mL Tris HCl 6.8 pH 0.5 M, 67.5 mL H_2O and 0.8 mL β -mercaptoethanol). It is then thoroughly washed with H_2O and incubated for 10 min at room temperature in mild stripping buffer (15 g glycine, 1 g SDS, 10 mL Tween20, volume brought up to 1 L with H_2O , and adjusted to 2.2 pH.). It is then washed with phosphate buffered saline (PBS) and TBST before proceeding with loading control detection.

Size Control As can be seen in Figure 1.2a, our data is consistent with our expectations: protein band slightly above 100 kDa, which is coherent both with the data specifications (1.2b) and with expected molecular weight: 92 kDa, without post-translational modifications, according to the manufacturer. U87 is our positive control, as is seen in the figure. There is only one important band around the expected size, which validates the quality of our antibody.

Normalization and quantification Our data is normalized using ImageJ software. Tubulin is used as an internal control for loading: the quantities of proteins

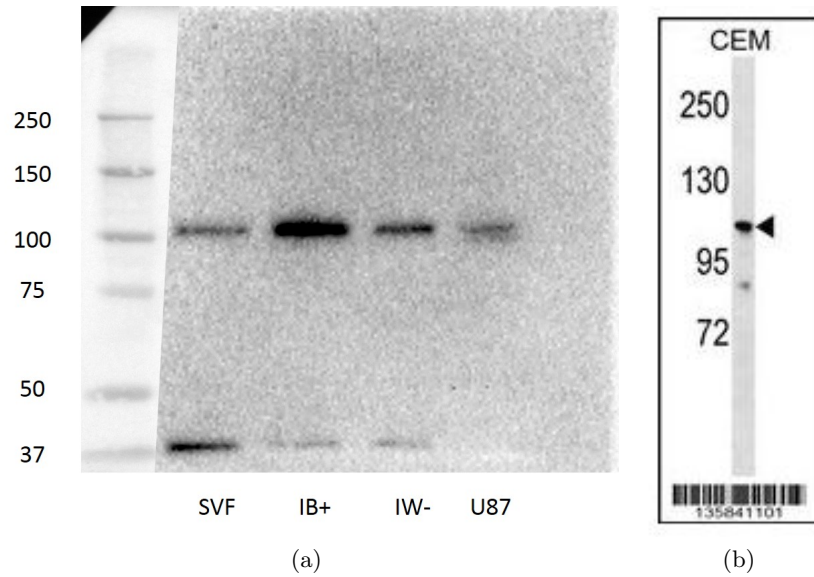


Figure 1.2: **Size control of the western blot** *Figure 1.2b* taken from the Raybiotech website

are first expressed as a ratio of expression compared to tubulin, and then fold-changes are calculated to the control of the experiment (SVF, MSC, IB+ or IW- as specified in the legend of the figure).

1.3.4 Alizarine Red staining

Fixation: Cells are fixated in 4% paraformaldehyde (PFA) in PBS for 10 min and rinsed 3 times. They can be stored in PBS at 4°C at that stage.

Staining: They are then incubated in filtrated Alizarine Red 2% in 4.1 pH for 5 min and washed 3 times with H_2O . Then are then left to dry and stored at 4°C. The well looks red if the osteoblast differentiation was successful (See Figure 1.3).

1.3.5 Mitochondrial oxygen consumption rate

Cells were seeded at usual density in XFe 24 cell culture plates (102340-100, XFe 24 FluxPak, Seahorse Bioscience, Chicopee, MA, USA). At the end of the differentiation protocol, cells are washed twice with XF assay medium (Seahorse Bio-

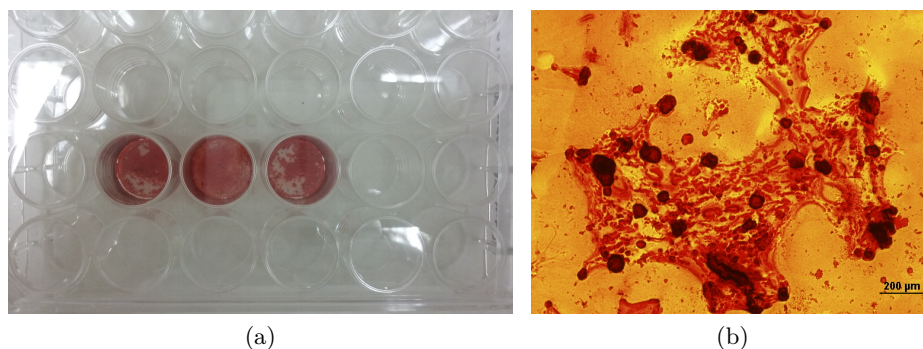


Figure 1.3: **Alizarine Red staining:** (a) Macroscopic view (b) Microscopic view

science, Chicopee, MA, USA), before a 20 min incubation at 37 °C in the absence of CO_2 in the same assay medium. The oxygen consumption rate (OCR) is then measured using the Seahorse XFe 24 analyzer (Seahorse Bioscience, Chicopee, MA, USA).

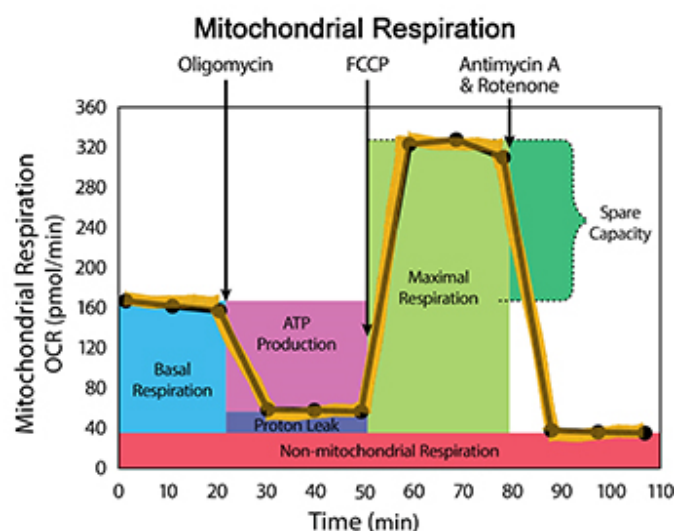


Figure 1.4: **Measuring the mitochondrial respiration:** *Figure taken from the Seahorse website*

10 μ M Forskolin (or DMSO as vehicle control) was added in order to stimulate the cells for 100 min. 2 μ M of Oligomycin, 0.6 μ M of carbonyl cyanide-4-(trifluoromethoxy) phenylhydrazone (FCCP), 2 μ M of rotenone and 2 μ M of Antimycin (XF Cell Mito Stress Test Kit, 101706-100, Seahorse Bioscience, Chicopee, MA, USA) were sequentially added in each well to differentiate the components con-

tributing to the total oxygen consumption of the cells of interest. The OCR before adding oligomycin is defined as mitochondrial respiration, the minimum OCR between addition of oligomycin and FCCP as uncoupled respiration, and the highest OCR after adding FCCP is defined as the total respiratory capacity (See Figure 1.4).

After those measurements, cells were lysed using $0.1 \text{ mg} \cdot \text{mL}^{-1}$ Proteinase K (P2308, Sigma-Aldrich, St-Louis, MO, USA). A solution of 10 mM Tris-HCl of 8.5 pH to 9.0 pH with 40 % glycerol was used to dissolve the enzyme to a concentration of $1 \text{ mg} \cdot \text{mL}^{-1}$. A lysis buffer (10 mM Tris-HCl (8.5 pH), 1 mM Ethylenediaminetetraacetic acid (EDTA), 0.1 % (v/v) Triton X-100) was used to dilute the enzyme to a working concentration of $0.1 \text{ mg} \cdot \text{mL}^{-1}$. The double-stranded DNA (dsDNA) content was measured using Quant-iT™ PicoGreen® dsDNA Kit (MP7581, Molecular Probes®, Life Technologies, Carlsbad, CA, USA), and the amount of dsDNA in each well was used to normalize OCR.

1.4 Immunostaining

1.4.1 TRPP3 and primary cilia staining

Fixation: After an ice incubation for 30 min in order to depolymerize non-acetylated microtubules, cells are rinsed twice in HBSS. Cells are then fixated in 4 % PFA in PBS for 7 min and rinsed thoroughly. They can be stored in PBS at 4 °C at that stage.

Permeabilisation: Cells are permeabilised in 3 % Triton X-100 (161-0407, BioRad, Hercules, CA, USA) in PBS for 3 min. Cells are then washed thrice with PBS.

Blocking: The basis solution used from now on is made of 3 % BSA in PBS

0.1 % Tween 20 (Sinopharm Chemicals, China). Cells are blocked for 30 min at room temperature.

Primary antibodies: The cells are incubated overnight at 4 °C in the basis solution supplemented with 1/2000 mouse anti acetylated tubulin (T-6793, Sigma-Aldrich, St- Louis, MO, USA) and 1/500 Rabbit anti-human PKD2L1 (102-12985, Raybiotech, Norcross, GA, USA).

Secondary antibodies: After washing twice with PBS, the cells are incubated 1 h at room temperature in the basis solution supplemented with 1/400 488 chicken anti-mouse (A21200) (Green) (A21200, Life Technologies, Carlsbad, CA, USA), 1/400 594 goat anti-rabbit (Red) (A11072, Life Technologies, Carlsbad, CA, USA) and 1/1000 4',6-diamidino-2-phenylindole (DAPI). The cells are then rinsed twice with PBS and can be stored in PBS at 4 °C.

Imaging: The cells are imaged using a confocal microscope from Yong Loo Lin School of Medicine, National University of Singapore, Confocal Microscopy Unit, unless stated otherwise.

Image analysis: The co-localisation coefficients were obtained using ImageJ Coloc2 plugin, and the analysis automated by a macro that I designed.

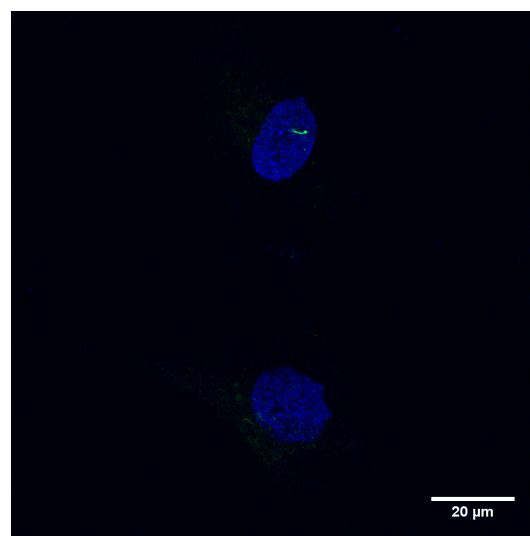


Figure 1.5: **Primary cilia staining.** In blue, DAPI staining. In green, acetylated tubulin staining.

1.4.2 Automated analysis

The ImageJ Coloc2 plugin allows to calculate different coefficients often used in biochemical studies of co-localization. A few steps were automatized in this process: a first macro was written to transform the images from oib format, given by the confocal microscope, to a RGB image that ImageJ can work with and a bright field image.

Then, a macro was written that took a folder of images that need to be analyzed and processed it with the following steps:

1. Calling the bright field image and manually assess the presence or not of lipid droplets to verify the state of differentiation
2. Calling the green image (acetylated tubulin) to verify the presence of primary cilia
3. Calling the red (TRPP3) and blue (DAPI) images to verify whether the probes seem co-localized and to assess the quality of the image
4. If the image was of a good enough quality, the Coloc2 plugin was called and automatically calculated the two interesting Manders' coefficients as well as importing the comments made by the plugin
5. The results were exported to an Excel file

Chapter 2

Investigating the presence of TRPP3

TRPP3 is a receptor from the TRP family, that has not been studied previously in adipocytes, either differentiated from SVF or MSC. We therefore decided to characterize it in those two cell types as a first step towards understanding its role.

2.1 Cellular characteristics of MSC and SVF

2.1.1 Definitions of MSC and SVF

The first step before comparing the expression of TRPP3 in those two cell types is to explain what they are.

The definition of MSC is given by the International Society for Cellular Therapy (See Dominici et al. (2006)). They have to verify three criteria:

1. *Plastic adherence*: Mesenchymal Stem Cells must be plastic adherent in standard *in vitro* conditions.
2. *Marker expression*: Those cells must verify the conditions presented in

Table 2.1.

3. *Differentiation potential*: MSC must be able to differentiate in adipocytes, osteoblasts and chondrocytes.

Marker	State	Role	Reference
CD 14 or <i>CD 11b</i>	Negative (≤ 2 %)	Immune system marker	Ziegler-Heitbrock and Ulevitch (1993), Kawai et al. (2005)
CD 19 or CD79 α	Negative (≤ 2 %)	Markers of β cells	Tedder and Isaacs (1989), Chu and Arber (2001)
<i>CD 34</i>	Negative (≤ 2 %)	Marker of primitive hematopoietic progenitors and epithelial cells	Satterthwaite et al. (1992)
<i>CD 45</i>	Negative (≤ 2 %)	Leukocyte marker	Altin and Sloan (1997)
<i>CD 73</i>	Positive (≥ 95 %)	Found on MSC. Converts Adenosine monophosphate (AMP) to adenosine	Tsukamoto (2014)
<i>CD 90</i>	Positive (≥ 95 %)	Marker of a wide range of stem cells	Wiesmann et al. (2006)
<i>CD 105</i>	Positive (≥ 95 %)	Found on MSC. Glycoprotein.	Maleki et al. (2014)
HLA-DR	Negative (≤ 2 %)	Human Leukocyte Antigen	Parham and Ohta (1996)

Table 2.1: **MSC markers** State represents the percentage of cells showing a marker expression. In *italic* are shown the markers common with SVF.

Those cells are extracted from bone marrow, where they share a stem cell niche with hematopoietic stem cells (Mendez-Ferrer et al. (2010)). Those cells, in culture, exhibit a fibroblastoid morphology (See Figure 2.1).

A definition of SVF was given in a joint statement by the International Federation for Adipose Therapeutics and Science and the International Society for Cellular Therapy (See Bourin et al. (2013)). We will call SVF what they define as adherent stromal cell, as the plastic-adherent sub-group of SVF. Therefore, the following criteria apply:

1. *Plastic adherence*: Stromal Vascular Cells must be plastic adherent in

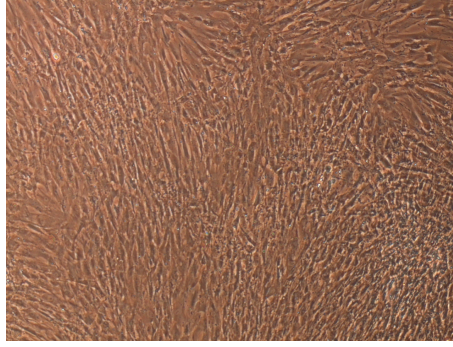


Figure 2.1: **MSC in culture.** Bright field image, $\times 4$ magnification

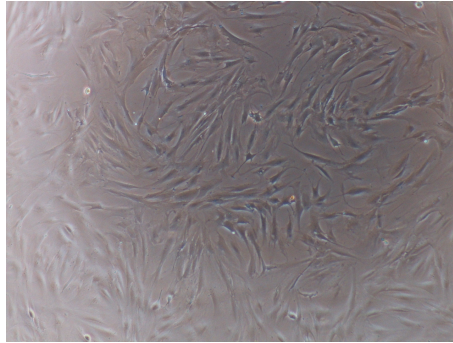


Figure 2.2: **SVF in culture.** Bright field image, $\times 4$ magnification

standard *in vitro* conditions.

2. *Marker expression:* Those cells must verify the conditions presented in Table 2.2.
3. *Differentiation potential:* SVF must be able to differentiate in adipocytes, osteoblasts and chondrocytes.

SVF are extracted from subcutaneous adipose, ubiquitous and easily accessible depots with a minimal invasive procedure (by liposuction aspiration) (Baer and Geiger (2012)). Several investigations encouraged the hypothesis of a perivascular localization of SVF within the fat tissue. Those cells, in culture, exhibit a fibroblastoid morphology (See Figure 2.2).

For more information on patients' characteristics, see 1.1.1.

Marker	State	Role	Reference
<i>CD 11b</i>	Negative (≤ 2 %)	Immune system marker	Kawai et al. (2005)
CD 13	Positive (≥ 90 %)	Marker of the myeloid lineage	Winnicka et al. (2010)
CD 29	Positive (≥ 90 %)	Integrin	Xue et al. (2015)
CD 31	Negative (≤ 2 %)	Platelet endothelial cell adhesion molecule	Xue et al. (2015)
<i>CD 34</i>	Present at variable levels	Marker of primitive hematopoietic progenitors and epithelial cells	Satterthwaite et al. (1992)
CD 44	Positive (≥ 90 %)	Cell-surface glycoprotein	Kang et al. (2013)
<i>CD 45</i>	Negative (≤ 2 %)	Leukocyte marker	Altin and Sloan (1997)
<i>CD 73</i>	Positive (≥ 90 %)	Found on MSC. Converts AMP to adenosine	Tsukamoto (2014)
<i>CD 90</i>	Positive (≥ 90 %)	Marker of a wide range of stem cells	Wiesmann et al. (2006)
<i>CD 105</i>	Positive (≥ 90 %)	Found on MSC. Glycoprotein.	Maleki et al. (2014)
CD 235a	Negative (≤ 2 %)	Glycoprotein, marker of erythrocyte	Dahr et al. (1987)

Table 2.2: **SVF markers** State represents the percentage of cells showing a marker expression. In *italic* are shown the markers common with MSC. in **bold** are shown primary markers.

2.1.2 Differences between SVF and MSC

As mentioned previously, we are interested in brown and white adipose tissues, and clinical applications to counteract effects of obesity.

We therefore decided to conduct most experiments on both cell types: SVF are more clinically relevant, but MSC have higher reproducibility between experiments. For each new donor of cells, a quality control was made to check for their stemness, that is their ability to differentiate in osteoblasts, white and brown adipocytes.

Characteristic	MSC	SVF	Reference
Plastic ad- herence	Yes	Yes	2.1.1
Marker ex- pression	Similar	Similar	2.1.1
Trilineage differentia- tion poten- tial	Yes	Yes	2.1.1
Localization in the body	Young adults' bone marrow	Patients' liposuction aspi- rate	1.1.1
Way of procuring	Bought from com- pany	Obtained from hospital	1.1.1
Batch to batch differ- ences	Small, same lot from the company	High donor to donor vari- ability	1.1.1
Clinical rele- vance	Relevant	Higher clinical relevance due to extraction from donor and presence in the body	

Table 2.3: **Differences and similarities in cellular characteristics between SVF and MSC**

2.2 Characterization on SVF-derived cells

2.2.1 TRPP3 expression in trilineage differentiation

As was mentioned previously (See 2.1), SVF have the potential for trilineage differentiation, into the following lineages: osteoblasts, chondrocytes and adipocytes. To assess whether TRPP3 was adipocyte-specific or a marker of all those differentiated cells, I performed a PCR study in osteoblasts, adipocytes and chondrocytes. As we can see in Figure 2.3, there is no TRPP3 expression in undifferentiated cells, osteoblasts or chondrocytes. However, there is high expression, more than 60 fold more than in the control, in both types of adipocytes. There is high variance in this experiment on the result for brown cells, but this does not change the conclusion of this first experiment: TRPP3 is an adipocyte-specific marker, which allows us to do further experiments, to characterize this receptor in SVF-derived adipocytes. This experiment excludes the hypothesis that

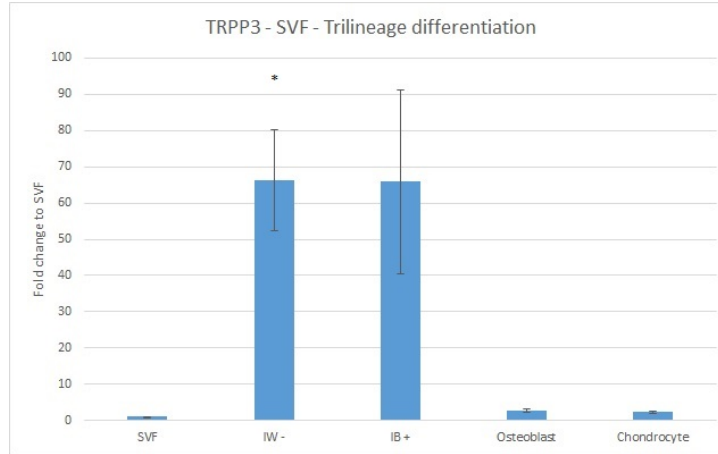


Figure 2.3: **Gene expression of TRPP3 presence in SVF-derived trilineage differentiated cells:** fold changes in reference to SVF. $n=3$ for each cell type. Significance is calculated compared to SVF. Not shown when not significant. *: $p<0.05$

TRPP3 is a maturity marker of stem cells, a marker to their loss of pluripotency or an age-related marker. The high standard deviation for both white and brown adipocytes do not allow us to compare the expression between those two lineages at the moment. The following study sought to differentiate the expression of TRPP3 in those two lineages: 2.2.2.

2.2.2 Characterization on the mRNA level

The first step in characterizing TRPP3 in SVF-derived adipocytes was to study its presence on the mRNA level. In order to do this, we decided to perform a qPCR (See Materials and Methods 1.2 for the protocol, and see Appendix 6 for primers references). We used TATA-binding protein (TBP) as a cDNA quantity control, and plot here the fold changes based on the CT values. This experiment was carried out by Anna Goralczyk, as there was high variability in the following batches of SVF that were used.

As can be seen in Figure 2.4a, the expression of TRPP3 varies according to the experimental conditions. As a reminder of what has been described in the Materials and Methods (1), SVF stands for non-differentiated cells, IW- for cells

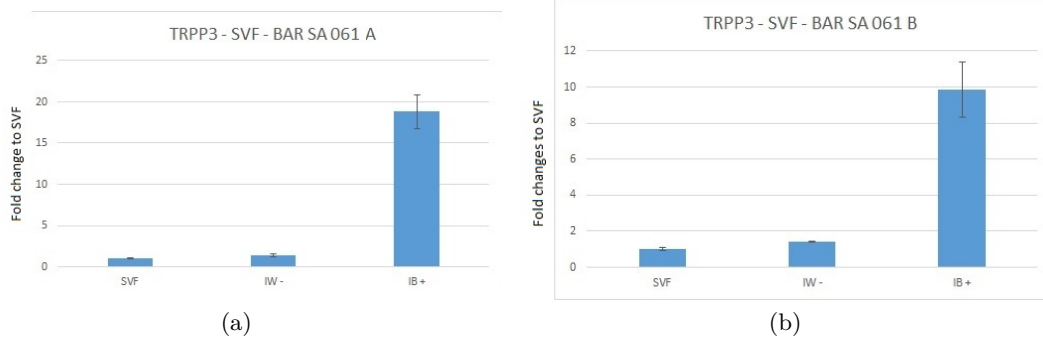


Figure 2.4: **Gene expression of TRPP3 in SVF-derived adipocytes** (a) First repeat on donor BARSA061. (b) Second repeat on donor BARSA061. $n=3$ for each cell type. Significance is calculated compared to SVF. Not shown when not significant. Results reproduced with permission from Anna Goralczyk.


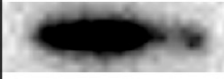

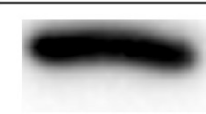
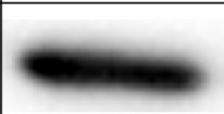

differentiated using the white differentiation protocol without macromolecular crowding (the cells expressing the least amount of UCP1 in our experiments), and IB+ stands for cells differentiated using the brown differentiation protocol with macromolecular crowding (the cells expressing the most amount of UCP1 in our experiments). SVF is used as a control, so its fold-change is defined as 1. We are therefore comparing expression levels to this level, knowing that since there is no Ct value for SVF, meaning the presence of TRPP3 cDNA is not detected by the machine, this means there is actually no expression of the gene. As we can see here, IW- cells express very low levels of TRPP3 mRNA, around the same level as undifferentiated SVF, which means there is very little TRPP3 in IW- cells. However, we can see that the fold change of TRPP3 in IB+ is around 18, which means it is much more expressed in those cells than in the other two cell types. The results are very similar for Figure 2.4b, where IW- levels are again close to SVF levels, meaning that there is almost no TRPP3 in IW- cells either. The fold change of TRPP3 in IB+ is around 10, which means it is much more expressed in those cells than in the other two cell types. This is lower than in the other repeat, but we are there only analyzing a trend, which is the same in both cell types.

The conclusion from this experiment on the gene expression level is that TRPP3 seems to be expressed in brown cells, and not in undifferentiated or white cells, on different repeats on the same experiment. Therefore, I decided to find out whether this was also true on the protein level, since a number of regulations intervene between the RNA expression and the presence of the functional protein in the cell.

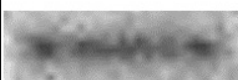

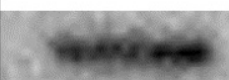



2.2.3 Characterization on the protein level

Since an up-regulation of TRPP3 in brown fat has been shown in the mRNA level, we decided to perform a Western Blot (WB) (See Materials and Methods 1.3 for the protocol) in order to assess whether or not this up-regulation was also reflected on the protein level. Since this protocol had not been used previously in the laboratory, I optimized it and verified the quality of the TRPP3 antibody using both the expected size control and a positive control.

As can be seen in Figure 2.5, the expression of TRPP3 varies according to the experimental conditions. As we can see here, SVF cells express very low levels of TRPP3 protein (which we assume to be basal levels), IW- express TRPP3 on an appreciably higher level, whereas IB+ express TRPP3 at an even higher level. To confirm those results, we decided to analyze this blot using ImageJ software, which allows for quantification of blots. Those results are presented in Figure 2.6, confirming what we saw on the blot: brown cells express TRPP3 protein at a higher level than SVF and white fat cells, around 3 times as much in one case. Run A does not show such a significant difference when analyzing the fold changes, even though we can see on the Western Blot that IB+ expresses TRPP3 on higher levels. We can still see the marked difference that existed between adipocytes and SVF on the gene level on the protein level.

TRPP3 SVF 061 A			
Condition	SVF	IB+	IW-
TRPP3			
tubulin			

(a)

TRPP3 SVF 061 B			
Condition	SVF	IB+	IW-
TRPP3			
tubulin			

(b)

Figure 2.5: **Protein expression of TRPP3 in SVF-derived adipocytes**
(a) First repeat on donor BARS061. (b) Second repeat on donor BARS061.
n=1 for each cell type.

The high levels of TRPP3 in IW- cells can be explained by the fact that their gene expression is slightly higher than SVF, which means there is translation of the proteins, and by the fact that some cells undergoing brown or white differentiation protocols still express characteristics from the other type of adipocyte.

This experiment proves that the up-regulation of TRPP3 that we saw at the mRNA level is also present at the protein level on SVF-derived brown adipocytes, and that TRPP3 is only present at a basal protein level on undifferentiated SVF. Now that we have characterized the TRPP3 expression at the end of the differentiation, as well as the correlation between mRNA and protein levels in

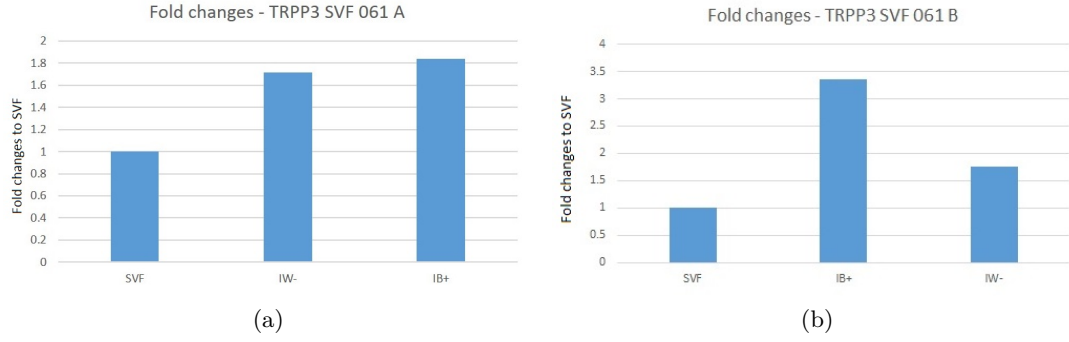


Figure 2.6: **Protein expression of TRPP3 in SVF-derived adipocytes (fold changes)** (a) Fold changes for the first repeat. (b) Fold changes for the second repeat.
n=1 for each cell type.

this cell line, I decided to characterize its time evolution, in order to see at what stage of differentiation it appeared.

2.2.4 Time evolution of TRPP3 presence

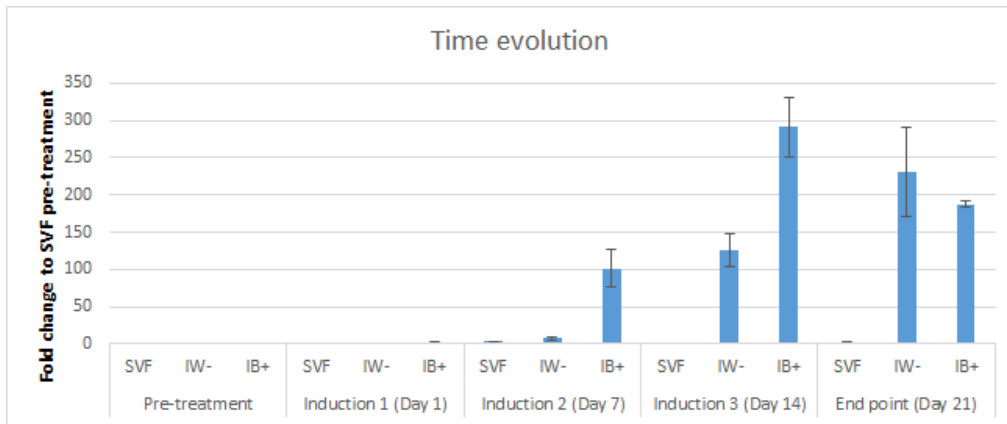


Figure 2.7: **Time evolution of the appearance of TRPP3 mRNA in SVF-derived cells:** gene expression using PCR on SVF, white and brown adipocytes.
n=3 for each cell type.

We can see thanks to these results that at induction 2 (see time-line 1.1 for more information), there is only little TRPP3 mRNA expressed, whereas it is highly present at induction 3, and close to the final levels it will reach at the end of culture. This is consistent with the PCR data presented in 2.2.2 up to induction 3. As mentioned in 2.1, there is high batch to batch variability in SVF

donors, and the donor used in this time evolution experiment did not differentiate correctly according to brown or white induction protocols, which does not put into question the time-line for its occurrence but only the comparison between IB+ and IW- TRPP3 expressions.

Now that we have fully characterized TRPP3 in SVF, we will also characterize it in MSC. This MSC study has been done before my arrival except for the protein data which I obtained.

2.3 Characterization on MSC-derived cells

2.3.1 Trilineage differentiation

As was mentioned previously (See 2.2.1), MSC, as SVF, have the potential for trilineage differentiation. This study was conducted before my arrival on MSC-derived cells, to prove that TRPP3 was adipose-specific and not present in the other SVF-derived lineages. (See 0.2.4). The absence of TRPP3 in other MSC-derived lineages allows for further characterization in MSC-derived adipocytes.

2.3.2 Characterization on the mRNA level

Just as for SVF-derived cells, the first step in characterizing TRPP3 in MSC-derived cells was to study its presence on the mRNA level. In order to do this, a qPCR study was carried out, that showed higher TRPP3 RNA expression in white adipocytes than in brown ones, contrary to the results obtained in SVF-derived cells, which will be analyzed more in depth in the next part 2.4.




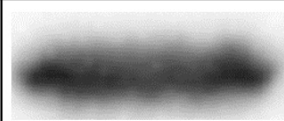
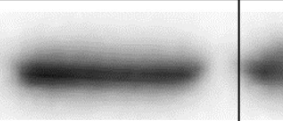
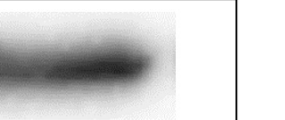
The conclusion from this experiment on the mRNA level is that TRPP3 seems to be highly expressed in white cells, expressed in brown cells, and not in undifferentiated cells, on different repeats on the same experiment. Therefore,

I decided to find out whether this was also true on the protein level, since a number of regulations intervene between the RNA expression and the presence of the functional protein in the cell. I thought a protein study was necessary before making any conclusions or hypothesis from the work that was done before my arrival.







2.3.3 Characterization on the protein level

Since an up-regulation of TRPP3 in white and brown fat has been shown in the mRNA level, I decided to perform a WB (See Materials and Methods 1.3 for the protocol) in order to assess whether or not this up-regulation was also reflected on the protein level.

As can be seen in Figure 2.8, the expression of TRPP3 varies according to the differentiation protocol used. MSC and IW- cells express low levels of TRPP3 protein, whereas IB+ express TRPP3 at a much higher level. To confirm those results, we decided to analyze this blot using ImageJ software, which allows for quantification of blots. Those results are presented in Figure 2.9, confirming what we saw on the blot: brown cells express TRPP3 protein at a higher level than MSC and white fat cells: around 2.7 times higher according to the fold changes presented in figure 2.9a, and around 2.2 times higher according to the fold changes presented in figure 2.9b. Those results are surprising at first, given the trend obtained on the mRNA level, which was opposite to the one obtained on the protein level, itself similar to the one obtained for SVF-derived cells. There are however a few explanations for this discrepancy between results on the mRNA and protein levels. First of all, we could be dealing with a receptor with a very long half-life, stabilized by interactions with other proteins for example. Therefore, a basal level even without detected mRNA signal can be expected.

TRPP3 MSC samples A			
Condition	MSC	IW-	IB+
TRPP3			
tubulin			

(a)

TRPP3 MSC samples B			
Condition	MSC	IW-	IB+
TRPP3			
tubulin			

(b)

Figure 2.8: **Protein expression of TRPP3 in MSC-derived adipocytes**
(a) First repeat. (b) Second repeat from the same donor.
n=1 for each cell type.

Another explanation is that there is some mRNA coding for TRPP3, but in very low quantities, such as to ensure only the renewal of the basal level of proteins that we see, and it is therefore not picked up by qPCR, which only detects higher signals. This mRNA could also have a very short life, which would explain why we cannot pick up a signal, except in some cell types where it is stabilized.

One last explanation resides in experimental issues: the primer could detect another gene (highly unlikely according to primerblast) or the antibody could detect the wrong protein (highly unlikely as it is at the expected size and there

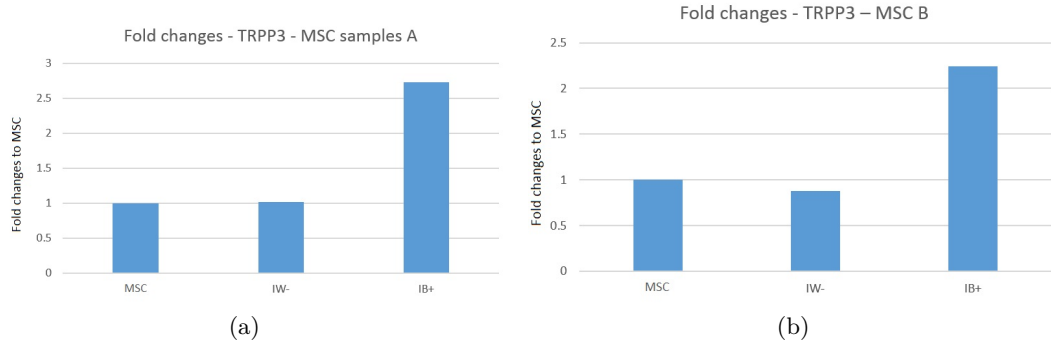


Figure 2.9: **Protein expression of TRPP3 in MSC-derived adipocytes (fold changes)** (a) Fold changes for the first repeat. (b) Fold changes for the second repeat from the same donor. *n=1 for each cell type.*

is a positive control).

Now that we have characterized the TRPP3 expression at the end of the differentiation, as well as compared the presence of mRNA and protein in this cell line, we can compare those results with its time evolution, in order to see at what stage of differentiation it appeared.

2.3.4 Time evolution of TRPP3 presence

It was found out that at induction 2 (see Time-line 1.1 for more information), there is still no TRPP3 mRNA expressed, whereas it is present at induction 3, and rising to its final levels during the last week of culture. This is consistent with the PCR data presented previously 2.3.2.

2.4 Conclusions

2.4.1 Similarities and differences between SVF and MSC

The time evolution analysis I conducted in SVF as well as the protein study I optimized and then led in SVF and MSC allowed me to summarize differences and similarities in TRPP3 expression between SVF and MSC in Table 2.4.

Characteristic	MSC	SVF
Trilineage differentiation	Present only in adipocytes	Present only in adipocytes
Gene expression	Higher in white adipocytes than in brown adipocytes	Higher in brown adipocytes than in white adipocytes
Protein expression	Higher in brown adipocytes than in white adipocytes	Higher in brown adipocytes than in white adipocytes
Consistency between those expressions	Discrepancy explained in 2.3.3	Yes
Time occurrence	Occurrence at induction 3	Earlier occurrence but at very low levels
Differences between repeats	Small between experiments	High between experiments, with the same trend between donors

Table 2.4: **Differences and similarities in TRPP3 expression between SVF and MSC**

2.4.2 Results analysis

Those results were interesting for various reasons. First of all, we have established that TRPP3 is present in adipocytes and not in undifferentiated cells, which make it an interesting topic of research in adipocytes. It is not a marker of stem cell aging, loss of pluripotency or stem cell maturity.

Secondly, we have established that it is regulated differently in brown and white cells, which makes it ever more interesting as our team is focused on the differences between those two types of adipocytes and the regulation of their differentiation.

We have also established a time evolution of the occurrence of this marker, which is not an age-related marker, as it is not present on undifferentiated cells, time-evolution which will be interesting for next planned experiments such as silencing.

Then, we have also established that those regulations are different on SVF

or MSC-derived cells, which means that analyzing both might lead to useful insights.

2.4.3 Choices for future experiments

Those results made me hypothesize that TRPP3 had a role in brown adipogenesis or functionality, as it is present in late differentiation stages and highly so in differentiated cells. Moreover, TRPP3 protein is present in much higher quantity in cells having undergone the brown differentiation protocol, which leads me to hypothesize its role in brown adipogenesis in particular rather than adipogenesis in general.

Given my results, I decided to further the study using both SVF and MSC. However, some of the experiments (such as localization and optimization) were conducted on SVF only. This is motivated for different reasons.

First of all, there is a direct correlation between WB and PCR data, which allows for easier analysis of results.

Secondly, SVF are cells with higher UCP1 expression, which that it will allow for more important reduction of its expression if our hypothesis about the role of TRPP3 as controlling brown differentiation in SVF-derived cells is true.

However, although SVF have more clinical relevance, as they are extracted directly from donors, they have higher batch to batch variation, as well as variations according to where the biopsy was made, which is why we decided to also conduct the silencing experiment on MSC.

For those different reasons, I decided to continue experiments on SVF-derived adipocytes for localization, optimization of protocols and silencing, while Anna Goralczyk used my protocols for study on MSC.

Chapter 3

Localization study

TRPP3 is a receptor that has been described in a few cell types, in different organisms, but never in adipocytes or SVF. First, I will describe its supposed localization according to existing literature, then present the results of the experiments that were carried out, and draw some conclusions from this study. All the experiments presented in this chapter were carried out in SVF-derived cells.

3.1 Expected localization

3.1.1 TRPP3's expected localization

DeCaen et al. (2013) showed that TRPP3, when interacting with PKD1-L1 through heteromeric pores, regulates calcium influx in the primary cilia (3.1.2). Other members of the Polycystic Kidney Disease (PKD) channels have been shown to interact with the primary cilia (Delmas (2005), Zhou (2009)). Studies looking into the regulation of TRPP3 by various conditions (heat, voltage, or alkalization to cite a few) use over-expression techniques, and find a membrane localization, which is not contradictory with a cilia localization since TRPP3 is over-expressed (Shimizu et al. (2009), Shimizu et al. (2011) and Higuchi et al.

(2014)). Therefore, we decided to investigate whether or not TRPP3 was co-localized with the primary cilia, whose role in adipocyte differentiation has been studied (3.1.2), or whether or not it was localized at the membrane of cells.

3.1.2 Primary cilia is involved in adipogenesis

Primary cilia is a solitary organelle, protruding from the cell surface above the centrosome, that senses cell environment thanks to its dense pool of receptors Phua et al. (2015). It is made of acetylated tubulin, which allows for its specific staining (See Materials and Methods for reference 1.5).

The suspected role of cilia in obesity and metabolic disorders has been detailed in Oh et al. (2015). Apart from a role in the hypothalamus and in regulation of food intake, increasing evidence points towards a role in adipogenesis itself. Mature adipocytes are unique vertebrate cells, as they are not thought to be ciliated. However, transient ciliogenesis could be fundamental to regulate adipogenesis (Marion et al. (2009)). When disturbing Bardet-Biedl syndrome (BBS) proteins that are necessary for ciliogenesis, adipogenesis is increased, showing a direct link between the primary cilia and adipogenesis (Marion et al. (2012)).

Another study of particular interest to our project was conducted by Qiu et al. (2010). They partially inactivated Polycystic Kidney Disease 1 (PKD1), member of a family known to interact with TRPP3 (Zheng et al. (2015)), and this activated adipogenesis in mouse bone marrow MSC. However, this proadipogenic effect of PKD1 inactivation was reversed by a partial decrease of another ciliary protein, Kinesin Family Member 3A (Kif3a). This proves that some ciliary proteins, known to form pores with TRPP3-like channels, are involved in controlling adipocyte differentiation, whether increasing or decreasing it. More-

over, the role of those ciliary proteins in regulating the balance between brown and white adipogenesis has not been elucidated yet. Therefore, we hypothesized that TRPP3 could be located at the primary cilia of adipocytes during differentiation: the role of cilia in adipogenesis is important and not elucidated, and known interaction partners of TRPP3 are located there.

3.2 Results of this localization study

3.2.1 No link between primary cilia and TRPP3 could be established

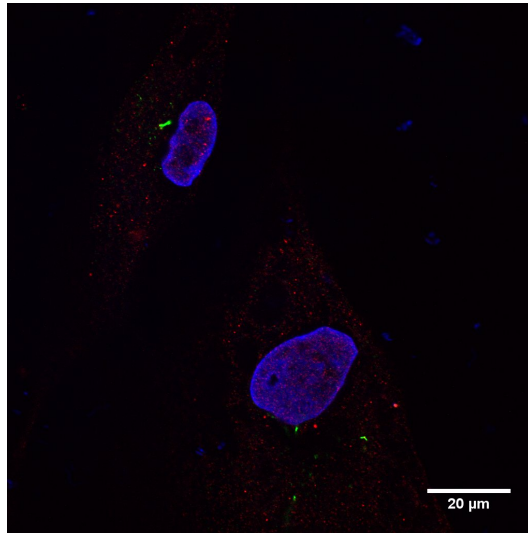


Figure 3.1: **Staining for TRPP3 of a ciliated cell** In blue, DAPI. In red, TRPP3. In green, acetylated tubulin. This cell was stained at T5 1.1 (beginning of maintenance 2), after undergoing an IB- differentiation protocol.

The protocol for cilia staining was adapted from Prosser and Morrison (2015), and optimized, as it was not done previously by the team. According to the literature review that has been presented in 3.1, we expected co-localization with primary cilia, which is not visible according to those images 3.1. We can see the primary cilia, a short and hair-like organelle, protruding from the cell, near the nucleus. This is coherent with a cilia' location, which is generated by

the centrosome. In this picture, the red staining corresponding to TRPP3 is present in the whole cytoplasm as well as in the nucleus. Therefore, we observe no co-localization in this picture. We chose this picture taken at T5 as it showed the cilia, which did not appear as clearly in later pictures. It was not observed in any of the cells presenting both cilia and TRPP3 staining. Therefore, this first hypothesis was abandoned. We then sought to establish whether localization of TRPP3 was dependent on differentiation protocol, and therefore dependent on the cell type.

3.2.2 No pattern of localization according to differentiation protocol was identified

Staining at the end of the differentiation period for different protocols is shown in Figure 3.2. The green channel represents acetylated tubulin, the component of cilia also present in the rest of the cytoskeleton. Here, no structure resembles a primary cilia. We can decipher cytoskeleton staining around the lipid droplets in Figure 3.2c. However, what is of most interest to us in this staining is the red channel, which represents TRPP3 staining. We can see in all pictures that there is very little or no staining in the cytoplasm of cells. However, a pronounced nuclear (DAPI, blue channel) stain is present in all cases. This study can therefore be deemed inconclusive, as the localization of TRPP3 is apparently the same after all differentiation protocols: brown differentiation with (see Figure 3.2a) or without crowding (see Figure 3.2b), white differentiation with (results not shown) or without (see Figure 3.2c) crowding or even basal levels in SVF (see Figure 3.2d).

Therefore, we have established that differentiation does not impact TRPP3 localization. However, those images suggest a novel localization for TRPP3, that

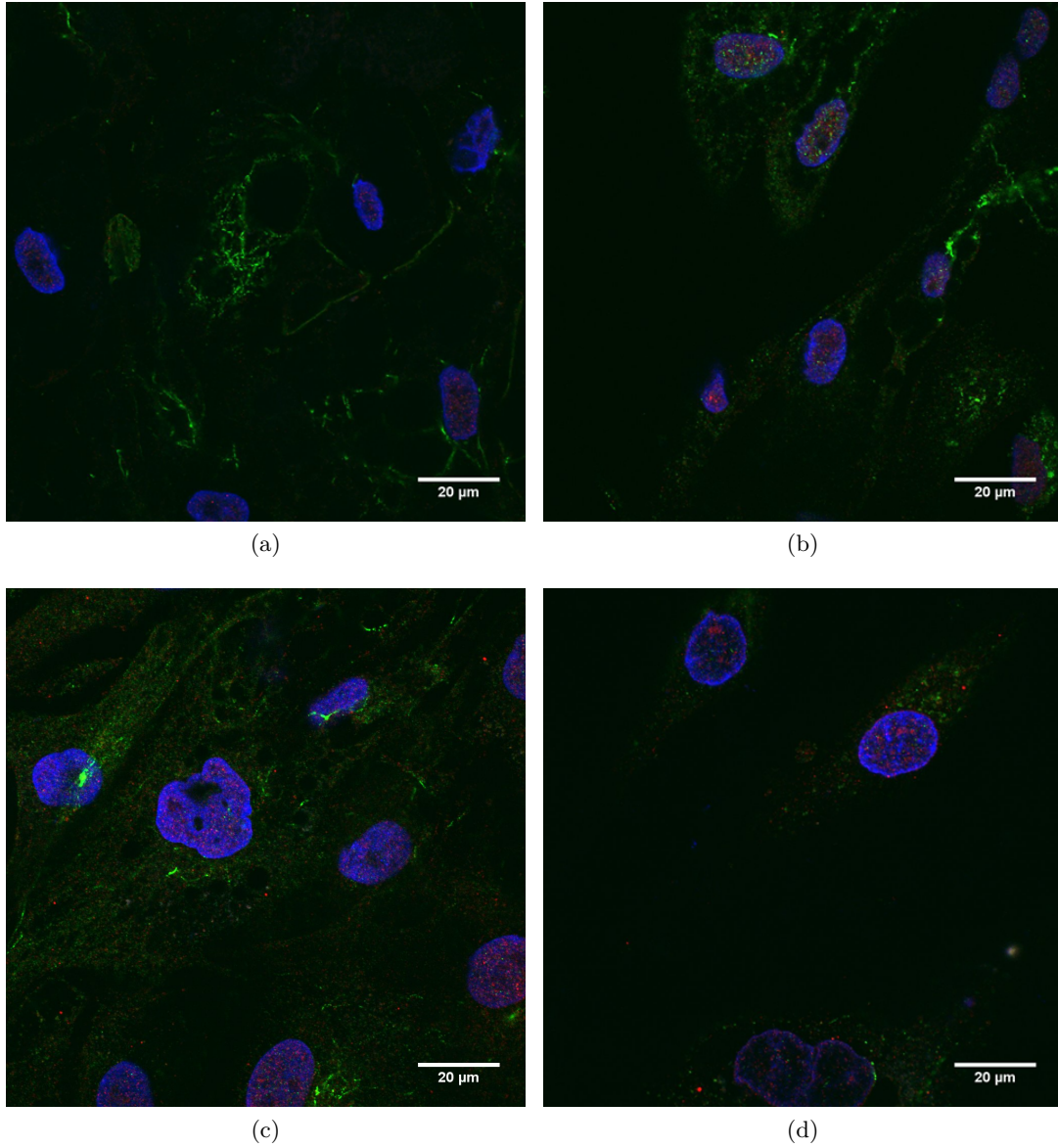


Figure 3.2: **Localization study at the end of differentiation** In blue, DAPI. In red, TRPP3. In green, acetylated tubulin. (a) Staining after full IB+ differentiation. (b) Staining after full IB- differentiation. (c) Staining after full IW- differentiation. (d) Staining after 3 weeks of SVF maintenance.

has not been reported in literature and is surprising given the protein sequence of TRPP3, as it seems that TRPP3 has a nuclear localization. Surprising as this nuclear localization may be according to known characteristics of TRPP3, we decided to investigate this hypothesis of a nuclear localization.

Some z-stack images were taken (results not shown) and it appears that the signal was not confined to the nucleus membrane but also present inside the nucleus. I then decided to run a co-localization analysis using the ImageJ Coloc2 plug-in (Dunn et al. (2011)), and more precisely using Manders' overlap coefficient.

3.2.3 Co-localization analysis

Two main techniques exist to quantify co-localization (See Dunn et al. (2011)), that do not make the same assumptions on the samples and probes.

The first one, called Pearson's correlation coefficient (PCC), takes the following form, taking as example red and green channels:

$$PCC = \frac{\sum_i (R_i - \bar{R}) \times (G_i - \bar{G})}{\sqrt{\sum_i (R_i - \bar{R})^2 \times \sum_i (G_i - \bar{G})^2}}$$

where R_i is the intensity value of the red channel for pixel i , G_i is the intensity value of the green channel for pixel i , and \bar{R} and \bar{G} refer to the mean intensities of those channels.

Therefore, PCC ranges from 1 where intensities are linearly correlated to -1 when they are inversely correlated. Values near 0 reflect distribution of probes that are uncorrelated to each other. Since there is a subtraction between the pixels and the mean intensity, this coefficient is independent of signal background or offset. However, despite its ease of use and other advantages, I chose not to

use this coefficient, as it is only adapted for probes that are linearly related to each other and that there is not reason in our study to have a linear correlation between our probes of interest.

The second technique, that I opted for, is called Manders' overlap coefficient (MOC), named after Manders who first published it (Manders et al. (1993)). Manders' coefficient is defined as follows:

$$MOC = \frac{\sum_i (R_i \times G_i)}{\sqrt{\sum_i R_i^2 \times \sum_i G_i^2}}$$

This coefficient is almost independent of signal proportionality, but is mainly sensitive to co-occurrence, that is the fraction of pixels that present high signals for both probes.

More precisely, we did not use MOC, but MCC (Manders' co-localization coefficient), characterizing the fractional overlap, that is the fraction of a probe that is co-localized with the other one. Those coefficients are simply calculated as:

$$MOC = \frac{\sum_i R_{i,colocal}}{\sum_i R_i}$$

where $R_{i,colocal} = R_i$ if $G_i > 0$ and 0 otherwise. Given that pixel values of 0 are rare if non-existent in microscopy, the image needs to be go through a first threshold-making step before being analyzed. Given the technique that we used to image and to threshold, there is not quantification possible between samples, it is only meaningful to see whether those values are high or low, but comparing numerical values between samples is not correct.

A technique has been developed to threshold images removing user bias for calculating those coefficients. The coefficients I am showing are therefore either without threshold or with Costes method (See Dunn et al. (2011)).

3.2.4 Manders' analysis

This process was automatized and all taken images went through this analysis process (see 1.4.2 for more details). The results are presented in Figure 3.3. We consider values to be significant when this coefficient is above 0.8 (co-localization) or below 0.2 (the probes are not co-localized), which means that no result here is significant. There is a difference between IB+ and IW- that could be considered numerically significant. However, the standard error plotted here does not take into account staining and imaging variations, which render this result insignificant, as it only takes into account the value given by the plug-in.

In this study, Manders' overlap coefficient 2 represents the fraction of TRPP3 that is co-localized with DAPI.

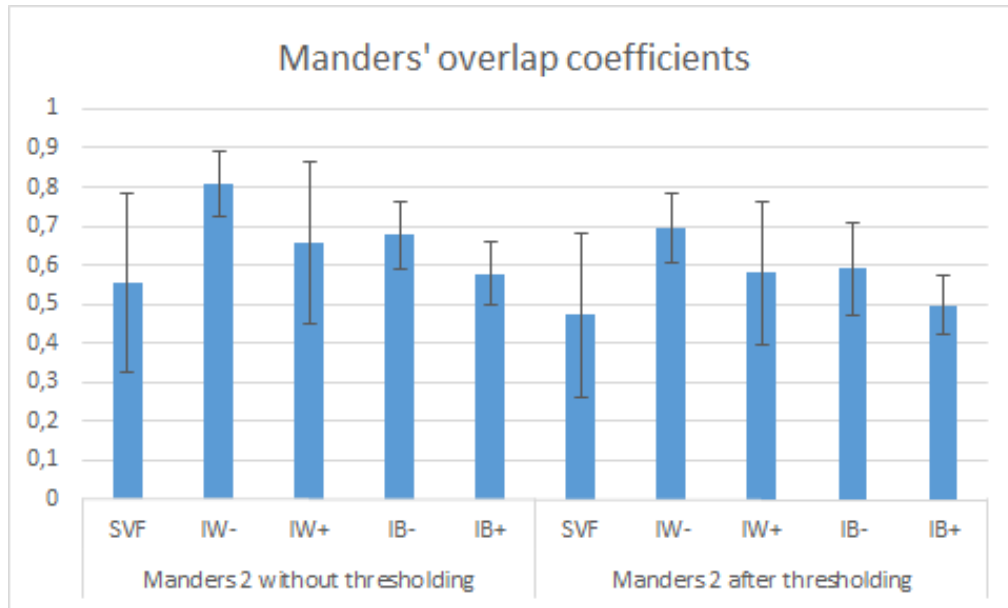


Figure 3.3: **Manders' overlap coefficient:**

The number of cells and images used are presented in Table 3.1. Significance is calculated compared to SVF. Not shown when not significant.

	SVF	IW-	IW+	IB-	IB+
Number of cells	48	84	61	112	96
Number of images	14	20	22	26	29

Table 3.1: **Mander's analysis:** number of cells and images used in the automated analysis

3.2.5 Different staining patterns were observed without any correlation to expected parameters: time or differentiation protocol

Even if the previous study (3.2.2) had been conclusive, other patterns obtained during the staining would have shed some doubts on the results. Those are presented in Figure 3.4. We can see in Figure 3.4a (Brown differentiation protocol plus crowding, after the first induction) a light staining in the cytoplasm that could be background, and a nuclear staining by very small aggregates. In Figure 3.4b (Brown differentiation protocol plus crowding, after two weeks of differentiation protocol), TRPP3 staining is dispersed in the cytoplasm. The same protocol with the same cells further in the plate gives very different results in Figure 3.4c: there is a very important nuclear staining, with little or no cytoplasmic background. We can see in Figure 3.4d (White differentiation protocol without crowding, after the third induction) a strong nuclear staining by aggregates.

As shown in Figure 3.4, very different staining patterns were observed, even in the same staining conditions as in 3.4b and 3.4c. Those do not follow any distinguishable pattern, whether depending on time or differentiation, as could have been expected.

3.3 Conclusions

3.3.1 Results are inconclusive

No link between primary cilia and TRPP3 could be established (3.2.1). No pattern of localization according to differentiation protocol was identified (3.2.2), and, surprisingly, different staining patterns were observed without any correla-

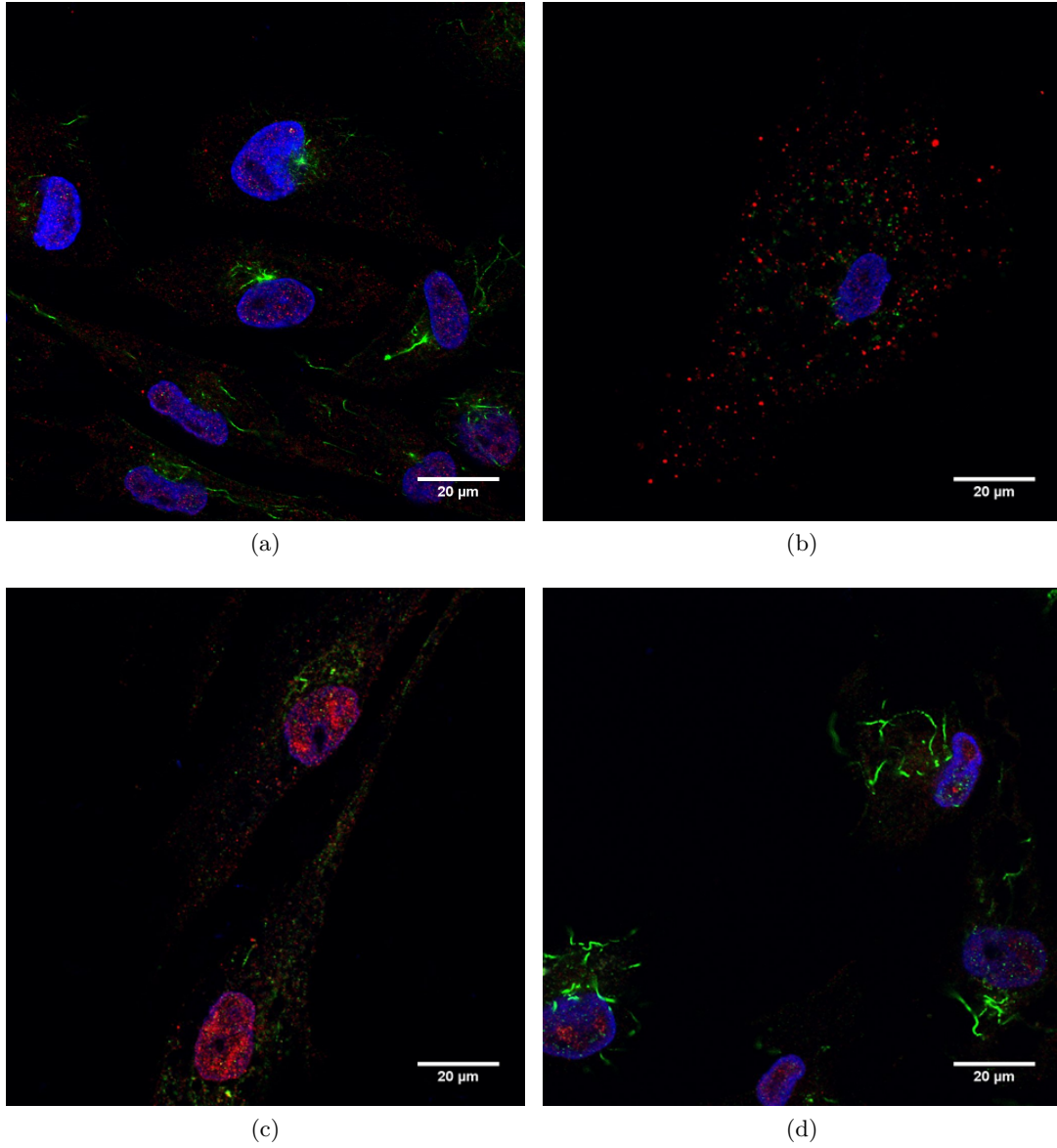


Figure 3.4: **Different staining patterns were presented** In blue, DAPI. In red, TRPP3. In green, acetylated tubulin. (a) Staining after induction 1 of IB+ differentiation. (b) Staining after maintenance 2 of IB+ differentiation. (c) Staining after maintenance 2 of IB+ differentiation. (d) Staining after induction 3 of IW- differentiation.

tion to expected parameters: time or differentiation protocol (3.2.5). The results of this study are therefore deemed inconclusive.

3.3.2 How do we account for those inconclusive results?

A few explanations exist for those results. The first one is that the antibody might not have been fit for immunochemistry. According to manufacturer's instructions, this antibody was meant for western blot analysis, and no mention of histochemistry was made in the data sheet. However, according to protein banks, it should stain an intracellular domain of the receptor, which is why we tried this experiment nonetheless. A nuclear localization is however consistent within most our samples, so one explanation is that those results, surprising as they might be, are actually true and TRPP3 is at the nucleus. We decided not to investigate this path of research further and focus on other studies which could give us a more direct insight into TRPP3's role.

Chapter 4

TRPP3 silencing study

Two methods are useful to understand the effect of a gene: either repressing it or over-expressing it, and to study more specifically a receptor, to block it or over-activate it. Since there is no known agonist or antagonist of TRPP3 available on the market as of yet, we decided to do interfere with the gene expression instead of with the receptor directly. However, since over-expressing the gene would necessitate plasmid transplantation, this is not feasible in a primary cell culture where cells loose differentiation potential after a few passages. We therefore decided to silence TRPP3 expression using the SiRNA method.

4.1 Principle of silencing

Adipocytes are known to be hard to transfect (Kilroy et al. (2009)), one of the main reasons being that only dividing cells are prone to transfection whereas adipocytes do not proliferate.

4.1.1 Lipofectamine transfection

The idea to use cationic lipids for transfection was expressed in 1987 (Felgner et al. (1987)), and has been further researched (Felgner et al. (1994)) and com-

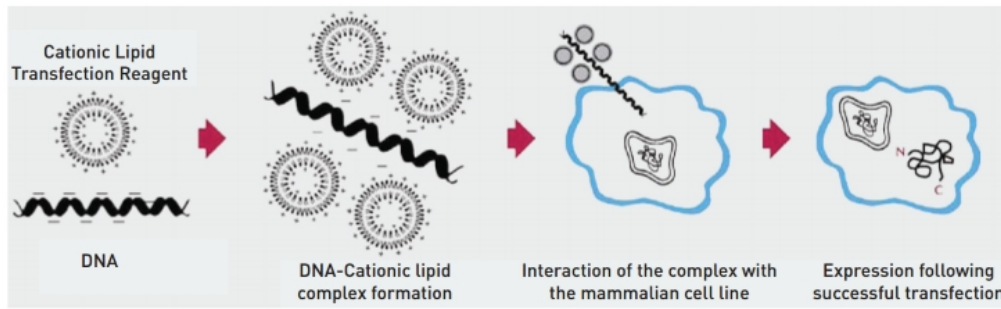


Figure 4.1: **Lipofectamine transfection principle** *Figure obtained from the Thermo Fisher website*

mercialized since. The principle of the technique, as illustrated in 4.1, is the following: since nucleic acid polymers (RNA,DNA) are anionic, they can form complexes with cationic lipids. These lipids, of a composition close to a cell' membrane, as they are both made of phospholipid bilayers, can then merge with the cell membrane, bringing the nucleic acid polymer into the cell' cytoplasm. The cell can then read this material and produce the desired effect (silencing, protein production or gene editing).

This allows us to understand the different steps of the silencing protocol (1.1.8):

1. *Lipofectamine incubation in media*: The aim of this step is to ensure that Lipofectamine assembles itself in lipid bilayers forming micelles, for 5 min.
2. *Lipofectamine and SiRNA incubation*: During this 20 min incubation, the SiRNA and the Lipofectamine form complexes as illustrated in the second step of 4.1.
3. *Transfection*: Once these complexes are formed, we can proceed to transfection, adding these complexes to the culture media.

4.1.2 SiRNA and PCR primers design

Once we have chosen the transfection method, we still have two questions: what SiRNA should we choose and how are we going to ascertain that the silencing worked? Those two questions are, as we will see, closely linked.

PCR is not always the best readout for silencing: the mRNA is still produced and might still be amplified by the PCR cycle even though it might be destroyed by RNA interference before translation of the protein, and therefore will still be picked up by the PCR at normal level although the silencing is efficient.

However, the manufacturer advises on SiRNA kit instructions to measure the RNA knock-down of gene expression with PCR for the following reasons: "the measurement of protein levels, enzyme activity, or phenotype can vary widely depending on protein half-life, turnover rates, and other factors such that it is possible to observe a seemingly negative result even when mRNA levels have been substantially suppressed. Protein levels and phenotype effects can be assessed after it has been established that mRNA levels are reduced".



Figure 4.2: **TRPP3** sequence with SiRNA cutting sites and primers used

For those reasons, we decided to optimize our protocol by assessing mRNA levels, and to then confirm those results on the protein level in a second round. It is necessary to also assess the effect of silencing on the protein level because of the variability on the mRNA level according to its degradation rate. As has been shown in numerous studies (Holen et al. (2002), Shepard et al. (2005), Hahn et al. (2004), Holmes et al. (2010)), the distance between the SiRNA binding

site and the amplified sequence is of paramount importance: if the sequence flanked by the primers comprises the binding site, then this sequence will be cut thanks to RNA interference and the PCR will faithfully show the proportion of silenced cells compared to the control. If this sequence is close to the binding site, the mRNA will likely be degraded and the PCR will likely reflect the silencing efficiency. However, the further the amplified sequence is from the binding site, the likelier it is that the cut fragment will not be degraded and still be amplified, showing no impact on the PCR level, even though the gene is silenced.

We therefore decided to use the two SiRNA duplexes and the two primer sets as can be seen in Figure 4.2.

4.2 Optimization

The first step before using this method efficiently is to choose and optimize the transfection reagents. We decided to use a Lipofectamine[®] 2000-mediated transfection, as adipocytes are known to be hard to transfect and that this technique has been proven to work in that cell type (Guan et al. (2005), Oberkofler et al. (2002)).

We then decided to optimize the quantity of reagents, based on both manufacturers' instructions: they gave different concentrations for Lipofectamine[®] 2000 and SiRNA, which is why we used a range of SiRNA concentrations. The universal scrambler is used at C1, Lipofectamine=1/50 and the Lipofectamine control is Lipofectamine=1/50.

The results of this optimization study are given in figure 4.3. The fold changes are calculated using the IB+ control as a reference. We can see, in the column "Lipofectamine=1/50", that the lower the concentration of SiRNA, the higher the expression of TRPP3, or in other words the lower the repression. More

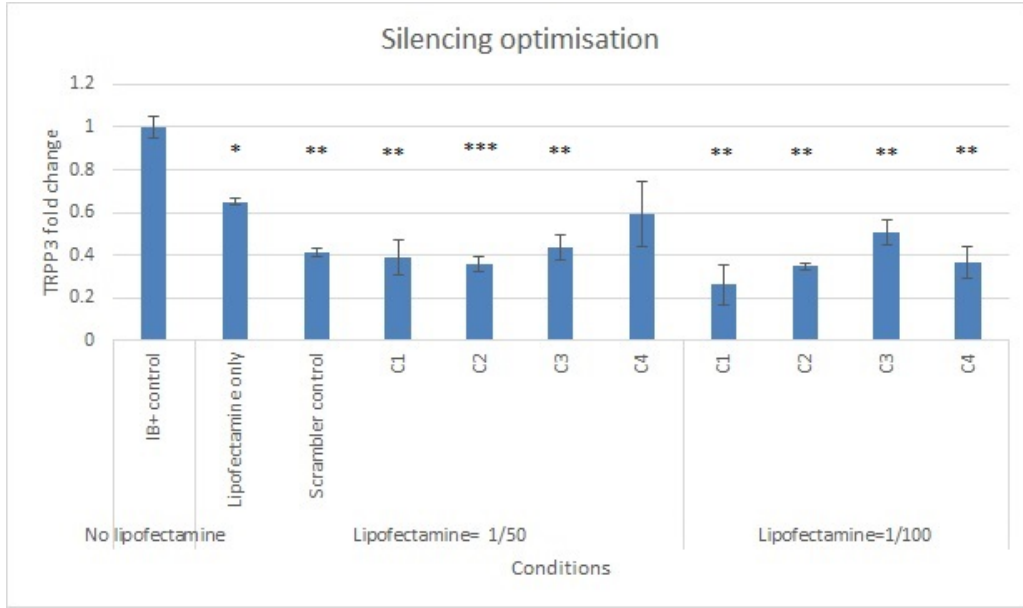


Figure 4.3: **Silencing optimization study:** PCR results for TRPP3, fold changes compared to IB+ differentiation

C1= 20 nM SiRNA

C2= 10 nM SiRNA

C3= 5 nM SiRNA

C4= 1 nM SiRNA

*n=3 for each cell type. Significance is calculated compared to IB+. Not shown when not significant. *: $p<0.05$. **: $p<0.01$. ***: $p<0.001$*

precisely, we can see a expression of TRPP3 expression around 40 % for C1= 20 nM, C2= 10 nM SiRNA and C3= 5 nM SiRNA, but an expression around 60 % for C4= 1 nM. This means that the repression of TRPP3 is around 60 % for C1, C2 and C3 but around 40 % for C4.

The lowest value for TRPP3 expression is obtained for C1 and Lipofectamine=1/100. This value is around 25 %, which is comparable to the maximum repression that could be guaranteed by the manufacturer. Therefore, we decided to use those concentrations for further experiments, as can be seen in 1.1.8.

In this experiment, the Lipofectamine and Universal Scrambler controls were not as close to the IB+ solution control as expected, since in the Lipofectamine control the TRPP3 expression is reduced by more than 30 %, and is around 40 % for the Universal Scrambler control, when they should not have affected TRPP3

expression.

Despite the surprising controls, we decided to proceed with experiments, as the repression we obtained with the chosen condition were close to the maximum we could hope for. The chosen experiments were

1. *Differentiation study*: we wanted to compare the effect of TRPP3 silencing on brown and white differentiations, as well as in SVF maintenance in culture (4.3.1)
2. *Functionality study*: we wanted to analyze the effect of TRPP3 silencing on brown fat function, as assessed by a Seahorse experiment (4.3.4)

These two experiments allow us to assess the role of TRPP3 in both adipocyte differentiation and function.

4.3 Results in SVF

After this optimization protocol was finalized, I proceeded to a study of the effect of silencing of TRPP3 on brown and white adipocytes differentiation on SVF cells.

4.3.1 Quality of differentiation

When using a batch of cells from a new donor, we first check the quality of their differentiation, by measuring UCP1 (brown marker) and leptin (maturity and white marker) expression. We can see in Figure 4.4 that with this donor, expressions in TRPP3, UCP1 and leptin are very similar, which means, given the high UCP1 expression, that both those differentiation protocols led to a majority of brown fat cells. Therefore, the discrepancy with previous results (2.4) is due to the propensity of this new batch to differentiate in brown fat cells, even under

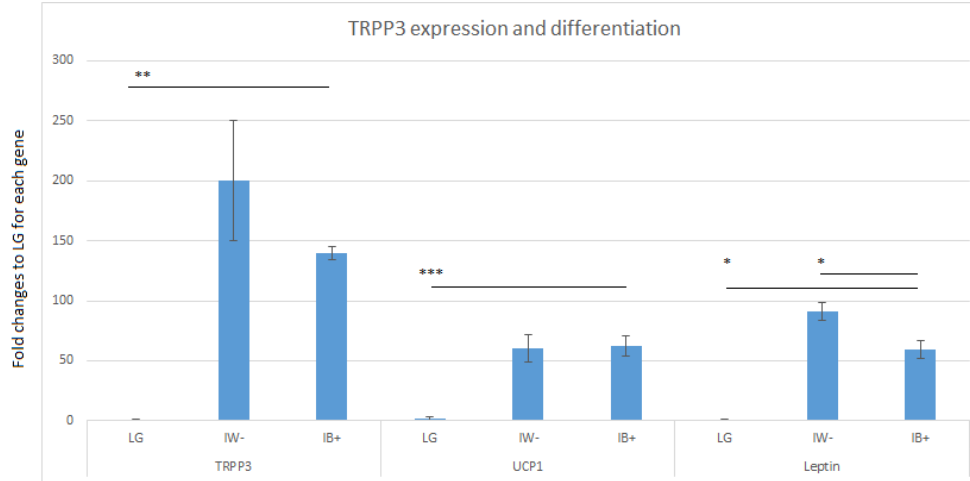


Figure 4.4: **Differentiation control of the silencing donor:** TRPP3, UCP1 and Leptin expressions in cells having undergone the following protocols: LG (low glucose, SVF cells), IW-: white adipocytes without macromolecular crowding, IB+: brown adipocytes with macromolecular crowding. $n=3$ for each cell type. Significance is calculated compared to IB+ for each gene. Not shown when not significant. *: $p<0.05$. **: $p<0.01$. ***: $p<0.001$

the IW- protocol. The TRPP3 expression levels are consistent with the UCP1 and Leptin expression levels. More explanations on this issue are given in the Discussion chapter 5.6.2.

4.3.2 Silencing of brown fat cells

Now that we have established that both differentiations seem to have led to brown fat cells, we are first going to study the effect of silencing of cells having undergone the IB+ differentiation protocol.

According to Figure 4.5a, we can see that our three controls (IB+ alone, IB+ and Lipofectamine and IB+ and Universal Scrambler) have similar levels of TRPP3. This shows that Lipofectamine and Universal Scrambler did not change TRPP3 expression, and that the effect of adding the SiRNA is due to the RNA interference and not the other reagents. We can see that TRPP3 expression is decreased in IB+ and SiRNA wells, although not to a significant level.

In 4.5b, we can see the mRNA levels in all precedent conditions, to under-

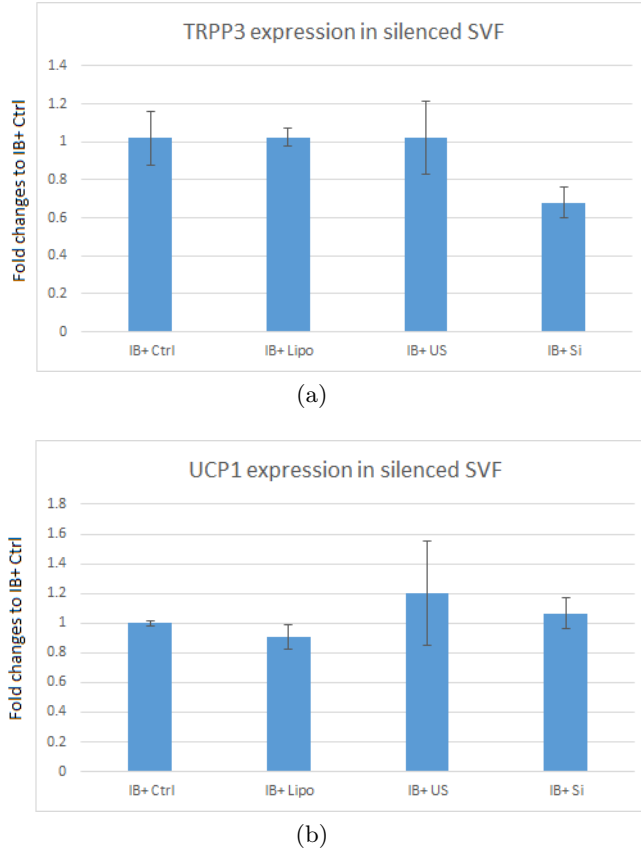


Figure 4.5: **TRPP3 and UCP1 gene expressions in silenced brown SVF:** (a) TRPP3 expression (b) UCP1 expression Ctrl: control, IB+ differentiation media, Lipo: Lipofectamine only, US: universal scrambler, Si: SiRNA-transfected cells.

n=3 for each condition. Significance is calculated compared to IB+ for each gene. Not shown when not significant.

stand the impact of TRPP3 silencing. We can see no effect of silencing in this experiment, as all conditions show the same level of UCP1. However, since the effect of silencing was not significant on TRPP3 level, this does not mean that TRPP3 silencing does not affect differentiation.

Therefore, we decided to also study the effect of silencing on the cells that went through the IW- differentiation protocol, since they expressed similar UCP1 levels as those which went through the IB+ protocol.

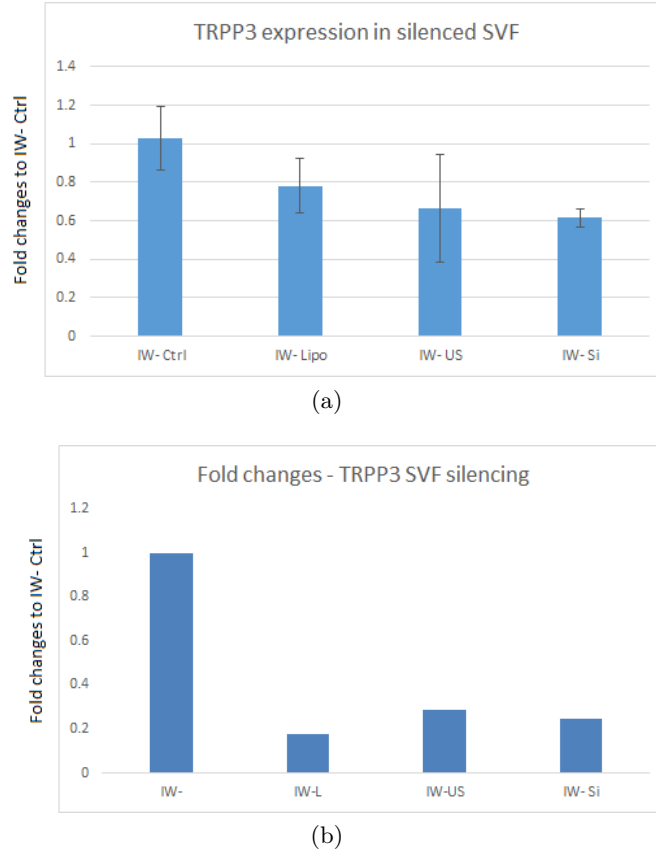
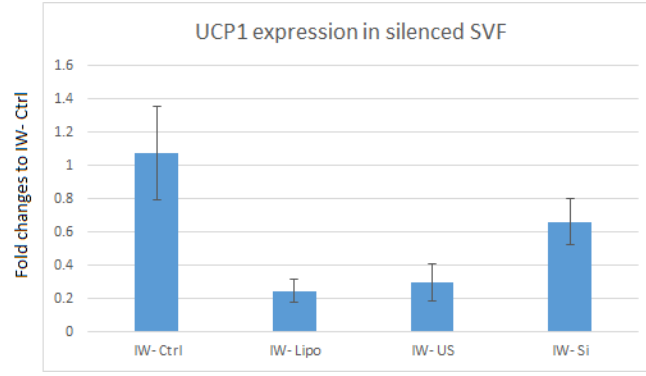


Figure 4.6: **TRPP3 gene and protein expression in silenced brown SVF:** (a) TRPP3 expression (gene) $n=3$ for each condition. Significance is calculated compared to IB+ for each gene. Not shown when not significant. (b) TRPP3 expression (protein) Ctrl: control, IB+ differentiation media, Lipo: Lipofectamine only, US: universal scrambler, Si: SiRNA-transfected cells.

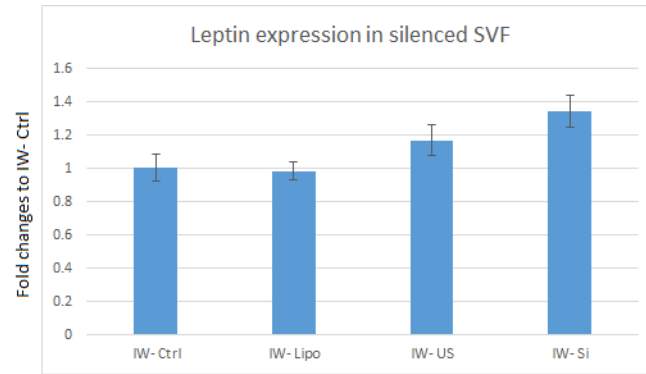
4.3.3 Silencing of white fat cells

According to Figures 4.6a and 4.6b, TRPP3 expression is reduced in silenced cells on the mRNA and protein levels (not significant). However, we can also see a decrease in the controls on both mRNA and protein levels, which means that Lipofectamine alone might influence TRPP3 expression. This will be further detailed in the Discussion section 5. What can be noted is that PCR and WB data are consistent, which means that even though we cannot deduct from this a causality between TRPP3 expression and differentiation, we will be able to deduct correlations.

We can see in Figure 4.7a that UCP1 levels are highly decreased in all con-



(a)



(b)

Figure 4.7: **UCP1 and leptin expressions in silenced brown SVF:** (a) UCP1 expression (gene) (b) Leptin expression (gene) Ctrl: control, IB+ differentiation media, Lipo: Lipofectamine only, US: universal scrambler, Si: SiRNA-transfected cells.

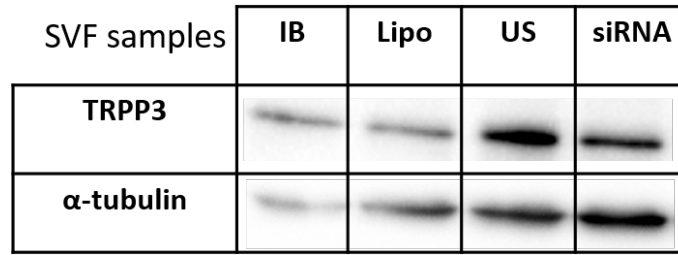
$n=3$ for each condition. Significance is calculated compared to IB+ for each gene. Not shown when not significant.

ditions where TRPP3 level was decreased. We can therefore see a correlation between TRPP3 and UCP1 expression. Leptin expression is also slightly higher in silenced white adipocytes than in the controls, (4.7b), which indicates that without TRPP3 cells seem to have more expression of white markers and less expression of brown markers.

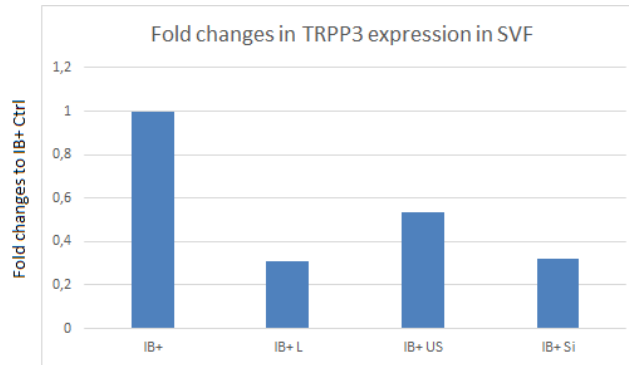
However, since the expression of the controls do not allow us to make any causality links but only correlations, we decided to reproduce this experiment on MSC, which have less batch to batch variability (See 4.4).

4.3.4 Effect on brown fat cells activity

We also decided to do a study of brown fat cells metabolic activity, to assess whether or not silencing of TRPP3 would allow for a change in cell metabolic activity despite the apparent lack of effect of UCP1 expression on brown fat cells. First, we verified the effect of silencing on TRPP3 protein levels. We had the same trend as with previous experiments on SVF: the controls with Lipofectamine and Universal Scrambler also show down-regulation compared to IB+ control. However, those results show that TRPP3 levels went down (See Figure 4.8).



(a)



(b)

Figure 4.8: **Effect of TRPP3 silencing in SVF** Ctrl: control, IB+ differentiation media, Lipo: Lipofectamine only, US: universal scrambler, Si: SiRNA-transfected cells (a) Protein expressions $n=1$ for each condition. (b) Fold changes in protein expression $n=1$ for each condition.

Once this down-regulation on TRPP3 protein expression was established, we performed a Seahorse experiment (See 1.3.5 for Materials and Methods). The aim of this experiment was to see the impact of TRPP3 silencing on mito-

chondrial respiration (the consumption of oxygen by mitochondria), respiratory capacity (their maximal consumption) and uncoupled respiration (also called proton leak, this is what corresponds to UCP1 activity and heat generation) in cells.

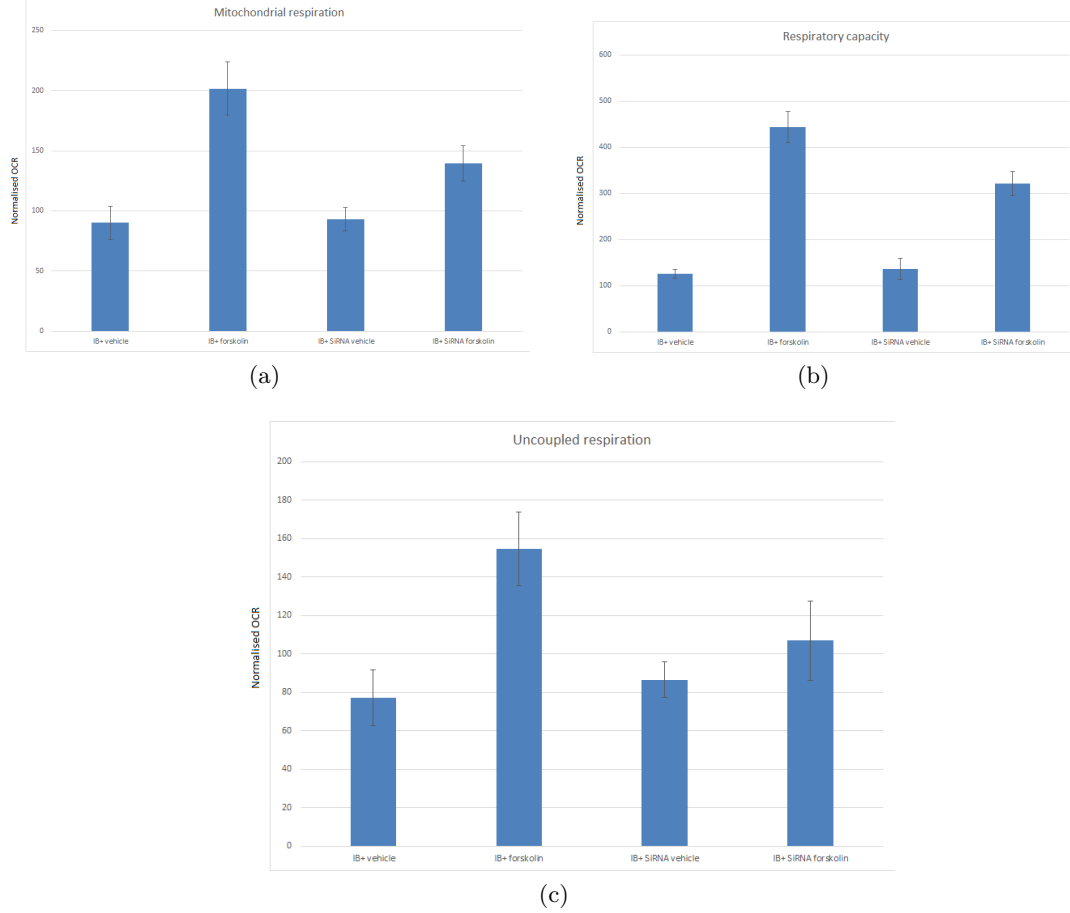


Figure 4.9: **Cell metabolic activity assessment in silenced SVF-derived brown adipocytes** Vehicle: DMSO loaded cells, Forskolin: forskolin loaded cells (a) Mitochondrial respiration (b) Respiratory capacity (c) Uncoupled respiration.

n=5 for each condition. Significance is calculated compared to IB+ for each gene. Not shown when not significant.

As we can see in Figure 4.9, there is a visible difference between IB+ and IB+ with SiRNA in respiratory capacity, mitochondrial and uncoupled respiration, although it is not significant. The most important one for our analysis, which concerns itself with the metabolism of brown fat, is the uncoupled respiration. This is responsible for heat generation by brown adipocytes. Even though the

results are not significant, their trend implies that TRPP3 silencing reduces brown fat metabolic activity, which means that TRPP3 would be necessary for brown fat activity. This could also be linked to the side effects of gene silencing, which were coupled with TRPP3 decrease in expression as shown in 4.8.

Since those results show a trend without proof, expression of the controls do not allow us to make any causality links but only correlations, we decided to reproduce this experiment on MSC (See 4.4). The effect on mitochondrial respiration showed the same trend as those presented here, but were significant (results not shown here).

4.4 Results in MSC

Despite those unconvincing results for SVF, Anna Goralczyk used the protocol I developed and optimized for SVF to transfect MSC, as those are less batch to batch dependent. I will briefly present those results as they support my study.

4.4.1 Effectiveness of silencing

There is no decrease in TRPP3 expression on the mRNA level in MSC, which can be explained easily as we are not using the same duplex for silencing MSC as we were using for silencing SVF, and this duplex is further away from the primer amplification site, which means that the degradation products can still be amplified by PCR (4.2 in the Principles of silencing section). This is why differentiation was also verified on the protein level: there is a decrease in TRPP3 expression on the protein level, confirming the effectiveness of my silencing protocol. This decrease is important (only 20 % protein expression of TRPP3 compared to the control), which means that results are more likely to be significant. Moreover, the Lipofectamine and Universal Scrambler controls presented similar levels as

IB+ only controls.

4.4.2 Influence on brown differentiation

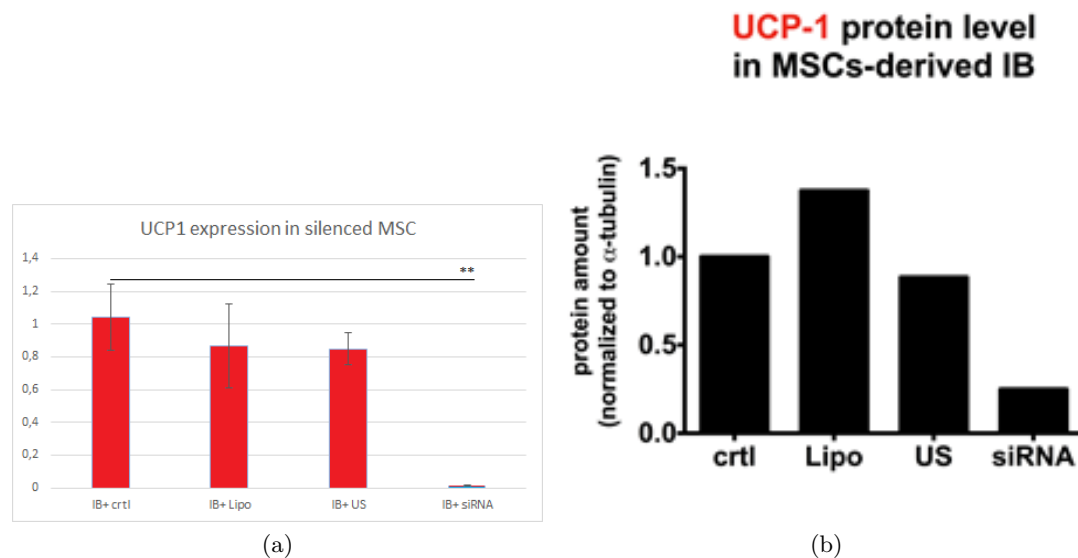


Figure 4.10: **Effect of TRPP3 silencing on UCP1 expression in MSC**
Ctrl: control, IB+ differentiation media, Lipo: Lipofectamine only, US: universal
scrambler, Si: SiRNA-transfected cells (a) Gene levels (b) Protein expressions
(c) Fold changes in protein expression. n=3 for each condition. *Courtesy of
Anna Goralczyk*

As shown in Figure 4.10a, UCP1 gene expression is similar for all the controls (IB+ alone, IB+ and Lipofectamine and IB+ and Universal Scrambler), and highly decreased (close to 77 fold decrease) for the silenced cells (1 % significance). Since all the controls (transfection reagent and universal scrambler) express similar levels of TRPP3 and UCP1 as the normal differentiation protocol, this decrease is due to the TRPP3 silencing. This is confirmed on the protein level (See Figure 4.10a and 4.10b), as this decrease is important (only 20 % protein expression of UCP1 compared to the control). We have therefore proven that TRPP3 silencing and decrease induces a decrease of similar importance in UCP1 expression in MSC-derived brown adipocytes.

Moreover, the Seahorse study (data not shown) shows that there is a signif-

ificant decrease in uncoupled respiration in silenced cells compared to the IB+ control, which confirms the trend that was obtained in SVF.

Chapter 5

Discussion

5.1 On the importance of understanding adipocyte differentiation

The global obesity problem is expected to become one of the most important health-related issues of the 21st century, as it is affecting hundreds of millions and this epidemics shows no sign of slowing down. As traditional prevention techniques have had only limited impact on this trend, finding ways to reduce the metabolic diseases related to obesity is becoming a crucial problem. Most current therapies tackle the symptoms and not the main cause of obesity, which is an energy imbalance between energy intake and energy consumption in the body. Linked to this are the two types of fat present in our body: white adipocytes which stores this excess of energy, and brown adipocytes which dissipate this extra energy as heat when stimulated. Understanding how those two cell types are linked and might switch from one to the other might give useful insights into the development of new drugs to target those cells.

5.2 Identification of TRPP3 as a target of interest

The TRP channels being of therapeutic interest, a study was conducted to identify which of these channels were present on adipocytes and whether they could be targets of interest.

5.2.1 TRPP3 is an adipocyte-specific marker

First, receptors that were up-regulated in adipocytes compared to undifferentiated cells were identified. Then, they were studied in osteoblasts and chondrocytes to ensure they were adipose-specific markers. No TRPP3 mRNA was detected in osteoblasts nor chondrocytes in both MSC (2.3.1) and SVF-differentiated (2.2.1) cells. This means that TRPP3 is adipose-specific, and is not a marker for loss of pluripotency or aging of stem cells.

5.2.2 TRPP3 is either a maturity or a brown adipocytes differentiation marker

Then, a time evolution study was carried out on both cell types. This shows that TRPP3 slowly appears during differentiation in both SVF and MSC-derived cells, under white and brown induction cocktails (2.3.4, 2.2.4). This means that TRPP3 could either be:

1. *A marker of adipocyte maturity:* this hypothesis would explain why TRPP3 is present in both white and brown differentiated cells, even though it would not explain the differences between the two types of adipocytes.
2. *A brown adipocytes differentiation marker:* this hypothesis would explain why TRPP3 is more highly present in brown adipocytes. The fact that it is also present in white-differentiated cells would then be explained by

the fact that some cells still express brown markers after ongoing a white differentiation protocol, as can be seen by their UCP1 expression (data not shown).

Further experiments were designed to opt between those two hypotheses.

5.3 Localization of TRPP3

Before characterizing further the role of TRPP3, we sought to localize it, as this often brings valuable information as to a receptor's role.

5.3.1 No visible pattern for the localization of TRPP3

As mentioned in 3.2, there is no visible pattern for TRPP3 localization, whether depending on maturity of differentiation or differentiation protocol. We therefore deemed this study inconclusive. According to literature on the topic, we were expecting it to be either co-localized with cells' primary cilia or with the cytoplasmic membrane. However, due to our results, it looked like TRPP3 could be localized at the nuclear membrane, which has not been mentioned in literature.

5.3.2 Calcium signaling is a key process in the nucleus

As reported in Santella and Carafoli (1997), Gomes et al. (2006) and Bootman et al. (2009), calcium signaling plays a vital role in the nucleus, a role that is not yet fully understood. It controls a number of nuclear function, from pore opening to gene expression, and the channels regulating it are not all identified as of yet.

5.3.3 TRPP3 could be a nucleus membrane channel

Therefore, although we did not decipher a pattern for TRPP3 localization, and we accepted that our results were inconclusive, further studies with better-characterized antibodies might find that TRPP3 is indeed a nucleus membrane channel, hypothesis that we rejected for the time being.

5.4 Characterizing the role of TRPP3

5.4.1 The silencing of TRPP3 in SVF is inconclusive

Although the results obtained in SVF cells (See 4.3) are not significant, they show some trends that will be discussed here. Due to high batch to batch variability among SVF donors, as well as a number of donors which cells did not differentiate as expected, those results were not reproducible.

After going through the usual IB+ differentiation protocol, TRPP3 silencing was not efficient and no result could be obtained on UCP1 expression for that reason. However, since the cells that underwent our IW- differentiation protocol exhibited brown cells features (similar levels of marker expressions), we decided to effect of silencing on that batch of cells. Important decrease of TRPP3 expression on the protein level was obtained in Lipofectamine, Universal Scrambler and SiRNA transfected cells, which we cannot explain at the moment. However, this correlates with a decrease in UCP1 expression and an increase in leptin expression, which leads us to hypothesize that TRPP3 is a marker of brown fat and that inhibiting or activating it could help switch from one phenotype to another.

Moreover, results from the metabolic activity assessment, although not significant either, imply that silencing TRPP3 reduces uncoupled respiration, char-

acteristic of brown adipocytes. The same results, but here conclusive, were obtained in MSC (data not shown in this study).

5.4.2 The silencing of TRPP3 in MSC helps discover a new role for TRPP3

In 4.4, we show that by silencing TRPP3, UCP1 is also reduced. Since the levels of UCP1 of all the controls are similar, we can deduce from this experiment that TRPP3 silencing is what reduces UCP1 levels. The trend is not as clear for Leptin, which is a maturity marker (and can also be considered a white marker, although this is questionable), since the controls are not as good as for UCP1. Therefore, we will only consider the effect of silencing on UCP1.

5.4.3 TRPP3 is not a maturity marker but is necessary for brown fat differentiation

The conclusion of this set of silencing experiments is that TRPP3 is necessary for brown fat differentiation, and might also be necessary for white adipocyte differentiation although our results are not entirely conclusive on that point. Therefore, we have identified a new receptor necessary for brown fat differentiation.

5.5 Pathways

Once we know that TRPP3 has an important role in brown fat differentiation, we then wondered what pathways it might act through.

5.5.1 Interaction with the cytoskeleton

It is known that cytoskeleton plays an important part in cellular functions and can control them (Chen et al. (1997)). In particular, the shape of mesenchymal stem cells can direct their differentiation into osteoblasts and adipocytes, as has been shown using micro-patterning techniques (McBeath et al. (2004), Kilian et al. (2010), Peng et al. (2011)). Thus, receptors known to interact with the cytoskeleton could use this effective pathway to influence cell fate. It has been proven that TRPP3 interacts with the cytoskeleton, either through α -actinin (Li et al. (2007)) or troponin I (Li et al. (2003)) and that this either up-regulates (actinin) or down-regulates (troponin) channel function. Therefore, more investigation is needed to understand the link between TRPP3 and the cytoskeleton, which is a promising way to uncover its pathway of action.

5.5.2 Calcium signaling in adipocyte differentiation

It has been established thanks to numerous studies that calcium signaling plays an important role in adipocyte differentiation, whether in early stages (Hu et al. (2009b), Hu et al. (2009a)) or at late stages of differentiation (Shi et al. (2000), Bishnoi et al. (2013)). Therefore, TRPP3 could control brown fat differentiation by modulating global calcium flux into the cells. The downstream effectors of that pathways are still to be identified.

5.5.3 Other pathways

receptor for activated C kinase 1 (RACK1) is a scaffolding/anchoring protein implicated in various cellular functions. In Yang et al. (2012), an interaction between the N-terminal domain of TRPP3 and RACK1 is established, and that this interaction inhibits TRPP3 channel function. Furthermore, a link has been

established between Wnt signaling and RACK1, as "RACK1 negatively regulates disheveled stability and Wnt signaling" (Cheng et al. (2016)), disheveled being a key component of the Wnt pathway. This pathway is known to be a key regulator in adipocyte differentiation, as Wnt signaling inhibits pre-adipocyte differentiation (Ross et al. (2000)).

5.6 Limitation of my study

5.6.1 Available tools to study TRPP3

The tools to study TRPP3 are still limited at this stage. Primer sequences for gene expression studies are easy to design using PrimerBlast, but antibodies for protein expression or immunochemistry are harder to obtain. Only two companies sell TRPP3 antibodies, and they do not allow for good immunochemistry, as has been shown in this study.

Then, to understand its function, only one tool is available: SiRNA silencing. Other methods exist but they are impossible to use for our study: there is no known agonist or antagonist of TRPP3 available, plasmid transplantation is only feasible in immortalized cell lines and we work with primary cells.

I therefore limited my study to the available tools and made the most of them.

5.6.2 Working with SVF

I also decided to work with SVF cells instead of MSC, as they are more clinically relevant. However, the very high variability between experiments, higher than what I expected, make MSC a better choice. This is especially true when working on brown and white adipocytes. Indeed, the SVF cells we use are obtained

from liposuction extracts. Since white, beige and brown adipocytes, as well as progenitors, are present in different amounts in different localizations within the adipose tissue, there would be high variability between samples extracted from the same patient. This means that with the same differentiation protocols, cells obtained from the same donor but from different localizations will present different ratios of brown and white adipocytes. This is even truer in samples obtained from different patients on different operations, which explains our high batch to batch variability. On the contrary, MSC are obtained from a company, and from the same donor for all repeats of our experiments. The experiments are therefore highly reproducible and might have been a better choice for a first study of this novel receptor, with the SVF study, more clinically relevant, in a second time. this is why MSC data is presented in this study alongside SVF data.

Conclusion and outlook

I studied the TRPP3 receptor in white and brown adipocytes in order to extend the toolbox for altering adipocyte differentiation.

TRPP3 is a member of the Transient Receptor Potential family, which have been shown to be sensitive to a wide range of stimuli. It has mostly been studied in the tongue as a potential sour receptor. It was identified by the team as having a different pattern of apparition in brown fat cells, which burn energy through uncoupling of the proton gradient, and in white adipocytes that store energy.

We first characterized extensively this apparition on two types of cells, SVF and MSC, in both white and brown adipocytes: time evolution, gene expression and protein expression. It was also shown that this was not present in other cells derived from those stem cells such as osteoblasts or chondrocytes, which means it would have been a stem cell maturity marker.

Then, we sought to localize it within cells, but this study was inconclusive, due to lack of adequate tools (antibodies) to effectively conduct this type of study at the moment. The localization we found was contradicting with existing literature and we decided to focus on other aspects of TRPP3 characteristics.

We then decided to understand its role by silencing its expression and see the impact on differentiation and function of cells. We proved that it was necessary

for brown adipocyte differentiation, as its silencing induced decreased levels of UCP1 and mitochondrial respiration.

To my knowledge, this is the first time TRPP3 was identified as being a key target in adipocyte differentiation.

5.6.3 Outlook

Further studies are needed to understand the pathways of action of TRPP3. Using arrays to identify up-regulated proteins between silenced and control cells is a promising way to identify those pathways.

To conclude, we find that greater attention should be devoted to identifying key regulators of adipocyte differentiation, in particular those controlling brown and white cell fate, as they will give more tools for clinicians to develop effective cell therapies.

Chapter 6

Appendix

Primers table

Gene	Accession no.	Sequence(5' - 3')	Reference
TBP	NM_003194.4	CACGAACCACGGCACTGATT TTTTCTTGCTGCCAGTCTGGAC	Spinsanti et al.
UCP1	NM_021833.4	CTGGAATAGCGGCGTGCTT AATAACACTGGACGTCGGGC	Virtanen et al.
TRPP3	NM_016112.2	ATCTGTCAAGGCATCAGAGGAC CAGATGTCCACCAGGAACACA	Virtanen et al.
Leptin	NM_000230.2	TTTGGCCCTATCTTTTCTATGTCC TGGAGGAGACTGACTGCGTG	Degawa Yamauchi et al.
FABP4	NM_001442.2	TGTGCAGAAATGGGATGGAAA CAACGTCCCTTGGCTTATGCT	Elabd et al.
GLUT4	NM_001042.2	TCAACAATGTCCTGGCGGTG TTCTGGATGATGTAGAGGTAGCGG	Lee et al.
CIDEA	NM_001279.3	GGCAGGTTACAGTGTGGATA GAAACACAGTGTTTGGCTCAAGA	Sharp et al.

Table 6.1: **Primers used in the study.**

Bibliography

- Ahern, G. P. (2013). Transient receptor potential channels and energy homeostasis. *Trends Endocrinol. Metab.*, 24(11):554–560.
- Altin, J. G. and Sloan, E. K. (1997). The role of CD45 and CD45-associated molecules in T cell activation. *Immunol. Cell Biol.*, 75(5):430–445.
- Ang, X. M., Lee, M. H., Blocki, A., Chen, C., Ong, L. L., Asada, H. H., Sheppard, A., and Raghunath, M. (2014). Macromolecular crowding amplifies adipogenesis of human bone marrow-derived mesenchymal stem cells by enhancing the pro-adipogenic microenvironment. *Tissue Eng Part A*, 20(5-6):966–981.
- Aquila, H., Link, T. A., and Klingenberg, M. (1985). The uncoupling protein from brown fat mitochondria is related to the mitochondrial adp/atp carrier. analysis of sequence homologies and of folding of the protein in the membrane. *EMBO J*, 4(9):2369–2376. 3000775[pmid].
- Baer, P. C. and Geiger, H. (2012). Adipose-derived mesenchymal stromal/stem cells: tissue localization, characterization, and heterogeneity. *Stem Cells Int*, 2012:812693.
- Bishnoi, M., Kondepudi, K. K., Gupta, A., Karmase, A., and Boparai, R. K. (2013). Expression of multiple Transient Receptor Potential channel genes in murine 3T3-L1 cell lines and adipose tissue. *Pharmacol Rep*, 65(3):751–755.
- Bonet, M. L., Oliver, P., and Palou, A. (2013). Pharmacological and nutritional agents promoting browning of white adipose tissue. *Biochim. Biophys. Acta*, 1831(5):969–985.
- Bootman, M. D., Fearnley, C., Smyrnias, I., MacDonald, F., and Roderick, H. L. (2009). An update on nuclear calcium signalling. *J. Cell. Sci.*, 122(Pt 14):2337–2350.
- Bourin, P., Bunnell, B. A., Casteilla, L., Dominici, M., Katz, A. J., March, K. L., Redl, H., Rubin, J. P., Yoshimura, K., and Gimble, J. M. (2013). Stromal cells from the adipose tissue-derived stromal vascular fraction and culture expanded adipose tissue-derived stromal/stem cells: a joint statement of the International Federation for Adipose Therapeutics and Science (IFATS) and the International Society for Cellular Therapy (ISCT). *Cytotherapy*, 15(6):641–648.
- Cannon, B. and Nedergaard, J. (2004). Brown adipose tissue: Function and physiological significance. *Physiological Reviews*, 84(1):277–359.
- Cao, W., Daniel, K. W., Robidoux, J., Puigserver, P., Medvedev, A. V., Bai, X., Floering, L. M., Spiegelman, B. M., and Collins, S. (2004). p38 mitogen-activated protein kinase is the central regulator of cyclic AMP-dependent

- transcription of the brown fat uncoupling protein 1 gene. *Mol. Cell. Biol.*, 24(7):3057–3067.
- Chen, C. S., Mrksich, M., Huang, S., Whitesides, G. M., and Ingber, D. E. (1997). Geometric control of cell life and death. *Science*, 276(5317):1425–1428.
- Chen, X. Z., Vassilev, P. M., Basora, N., Peng, J. B., Nomura, H., Segal, Y., Brown, E. M., Reeders, S. T., Hediger, M. A., and Zhou, J. (1999). Polycystin-L is a calcium-regulated cation channel permeable to calcium ions. *Nature*, 401(6751):383–386.
- Cheng, M., Xue, H., Cao, W., Li, W., Chen, H., Liu, B., Ma, B., Yan, X., and Chen, Y. G. (2016). RACK1 promotes Dishevelled degradation via autophagy and antagonizes Wnt signaling. *J. Biol. Chem.*
- Chu, P. G. and Arber, D. A. (2001). CD79: a review. *Appl. Immunohistochem. Mol. Morphol.*, 9(2):97–106.
- Clapham, D. E. (2003). Trp channels as cellular sensors. *Nature*, 426(6966):517–524.
- Dahr, W., Beyreuther, K., and Moulds, J. J. (1987). Structural analysis of the major human erythrocyte membrane sialoglycoprotein from Miltenberger class VII cells. *Eur. J. Biochem.*, 166(1):27–30.
- DeCaen, P. G., Delling, M., Vien, T. N., and Clapham, D. E. (2013). Direct recording and molecular identification of the calcium channel of primary cilia. *Nature*, 504(7479):315–318.
- Degawa Yamauchi, M., Moss, K. A., Bovenkerk, J. E., Shankar, S. S., Morrison, C. L., Lelliott, C. J., Vidal-Puig, A., Jones, R., and Considine, R. V. (2005). Regulation of adiponectin expression in human adipocytes: effects of adiposity, glucocorticoids, and tumor necrosis factor alpha. *Obes. Res.*, 13(4):662–669.
- Delmas, P. (2005). Polycystins: polymodal receptor/ion-channel cellular sensors. *Pflügers Arch.*, 451(1):264–276.
- Dewavrin, J.-Y., Abdurrahim, M., Blocki, A., Musib, M., Piazza, F., and Raghunath, M. (2015). Synergistic rate boosting of collagen fibrillogenesis in heterogeneous mixtures of crowding agents. *The Journal of Physical Chemistry B*, 119(12):4350–4358. PMID: 25730613.
- Dominici, M., Le Blanc, K., Mueller, I., Slaper-Cortenbach, I., Marini, F., Krause, D., Deans, R., Keating, A., Prockop, D. j., and Horwitz, E. (2006). Minimal criteria for defining multipotent mesenchymal stromal cells. The International Society for Cellular Therapy position statement. *Cytotherapy*, 8(4):315–317.
- Dunn, K. W., Kamocka, M. M., and McDonald, J. H. (2011). A practical guide to evaluating colocalization in biological microscopy. *Am. J. Physiol., Cell Physiol.*, 300(4):C723–742.
- Elabd, C., Basillais, A., Beaupied, H., Breuil, V., Wagner, N., Scheideler, M., Zaragosi, L. E., Massiera, F., Lemichez, E., Trajanoski, Z., Carle, G., Euler-Ziegler, L., Ailhaud, G., Benhamou, C. L., Dani, C., and Amri, E. Z. (2008).

- Oxytocin controls differentiation of human mesenchymal stem cells and reverses osteoporosis. *Stem Cells*, 26(9):2399–2407.
- Felgner, J. H., Kumar, R., Sridhar, C. N., Wheeler, C. J., Tsai, Y. J., Border, R., Ramsey, P., Martin, M., and Felgner, P. L. (1994). Enhanced gene delivery and mechanism studies with a novel series of cationic lipid formulations. *J. Biol. Chem.*, 269(4):2550–2561.
- Felgner, P. L., Gadek, T. R., Holm, M., Roman, R., Chan, H. W., Wenz, M., Northrop, J. P., Ringold, G. M., and Danielsen, M. (1987). Lipofection: a highly efficient, lipid-mediated DNA-transfection procedure. *Proc. Natl. Acad. Sci. U.S.A.*, 84(21):7413–7417.
- Gannier, F., White, E., Lacampagne, A., Garnier, D., and Le Guennec, J. Y. (1994). Streptomycin reverses a large stretch induced increases in $[Ca^{2+}]_i$ in isolated guinea pig ventricular myocytes. *Cardiovasc. Res.*, 28(8):1193–1198.
- Gomes, D. A., Leite, M. F., Bennett, A. M., and Nathanson, M. H. (2006). Calcium signaling in the nucleus. *Can. J. Physiol. Pharmacol.*, 84(3-4):325–332.
- Guan, H. P., Ishizuka, T., Chui, P. C., Lehrke, M., and Lazar, M. A. (2005). Corepressors selectively control the transcriptional activity of PPARgamma in adipocytes. *Genes Dev.*, 19(4):453–461.
- Hahn, P., Schmidt, C., Weber, M., Kang, J., and Bielke, W. (2004). RNA interference: PCR strategies for the quantification of stable degradation-fragments derived from siRNA-targeted mRNAs. *Biomol. Eng.*, 21(3-5):113–117.
- Higuchi, T., Shimizu, T., Fujii, T., Nilius, B., and Sakai, H. (2014). Gating modulation by heat of the polycystin transient receptor potential channel PKD2L1 (TRPP3). *Pflugers Arch.*, 466(10):1933–1940.
- Hilton, J. K., Rath, P., Helsell, C. V. M., Beckstein, O., and Horn, W. D. V. (2015). Understanding thermosensitive transient receptor potential channels as versatile polymodal cellular sensors. *Biochemistry*, 54(15):2401–2413. PMID: 25812016.
- Holen, T., Amarzguioui, M., Wiiger, M. T., Babaie, E., and Prydz, H. (2002). Positional effects of short interfering RNAs targeting the human coagulation trigger Tissue Factor. *Nucleic Acids Res.*, 30(8):1757–1766.
- Holmes, K., Williams, C. M., Chapman, E. A., and Cross, M. J. (2010). Detection of siRNA induced mRNA silencing by RT-qPCR: considerations for experimental design. *BMC Res Notes*, 3:53.
- Hu, H., He, M. L., Tao, R., Sun, H. Y., Hu, R., Zang, W. J., Yuan, B. X., Lau, C. P., Tse, H. F., and Li, G. R. (2009a). Characterization of ion channels in human preadipocytes. *J. Cell. Physiol.*, 218(2):427–435.
- Hu, R., He, M. L., Hu, H., Yuan, B. X., Zang, W. J., Lau, C. P., Tse, H. F., and Li, G. R. (2009b). Characterization of calcium signaling pathways in human preadipocytes. *J. Cell. Physiol.*, 220(3):765–770.

- Ishimaru, Y., Inada, H., Kubota, M., Zhuang, H., Tominaga, M., and Matsunami, H. (2006). Transient receptor potential family members PKD1L3 and PKD2L1 form a candidate sour taste receptor. *Proc. Natl. Acad. Sci. U.S.A.*, 103(33):12569–12574.
- James, P. T. (2004). Obesity: The worldwide epidemic. *Clinics in Dermatology*, 22(4):276 – 280. Obesity.
- Kajimura, S., Seale, P., Kubota, K., Lunsford, E., Frangioni, J. V., Gygi, S. P., and Spiegelman, B. M. (2009). Initiation of myoblast to brown fat switch by a PRDM16-C/EBP-beta transcriptional complex. *Nature*, 460(7259):1154–1158.
- Kang, H. S., Liao, G., DeGraff, L. M., Gerrish, K., Bortner, C. D., Garantzios, S., and Jetten, A. M. (2013). CD44 plays a critical role in regulating diet-induced adipose inflammation, hepatic steatosis, and insulin resistance. *PLoS ONE*, 8(3):e58417.
- Kawai, K., Tsuno, N. H., Matsushashi, M., Kitayama, J., Osada, T., Yamada, J., Tsuchiya, T., Yoneyama, S., Watanabe, T., Takahashi, K., and Nagawa, H. (2005). CD11b-mediated migratory property of peripheral blood B cells. *J. Allergy Clin. Immunol.*, 116(1):192–197.
- Kershaw, E. E. and Flier, J. S. (2004). Adipose tissue as an endocrine organ. *J. Clin. Endocrinol. Metab.*, 89(6):2548–2556.
- Kilian, K. A., Bugarija, B., Lahn, B. T., and Mrksich, M. (2010). Geometric cues for directing the differentiation of mesenchymal stem cells. *Proc. Natl. Acad. Sci. U.S.A.*, 107(11):4872–4877.
- Kilroy, G., Burk, D. H., and Floyd, Z. E. (2009). High efficiency lipid-based siRNA transfection of adipocytes in suspension. *PLoS ONE*, 4(9):e6940.
- Lee, E. K., Lee, M. J., Abdelmohsen, K., Kim, W., Kim, M. M., Srikantan, S., Martindale, J. L., Hutchison, E. R., Kim, H. H., Marasa, B. S., Selimyan, R., Egan, J. M., Smith, S. R., Fried, S. K., and Gorospe, M. (2011). miR-130 suppresses adipogenesis by inhibiting peroxisome proliferator-activated receptor gamma expression. *Mol. Cell. Biol.*, 31(4):626–638.
- Lee, M. H., Goralczyk, A. G., Kriszt, R., Ang, X. M., Badowski, C., Li, Y., Summers, S. A., Toh, S. A., Yassin, M. S., Shabbir, A., Sheppard, A., and Raghunath, M. (2016). ECM microenvironment unlocks brown adipogenic potential of adult human bone marrow-derived MSCs. *Sci Rep*, 6:21173.
- Li, Q., Dai, X.-Q., Shen, P. Y., Wu, Y., Long, W., Chen, C. X., Hussain, Z., Wang, S., and Chen, X.-Z. (2007). Direct binding of alpha-actinin enhances trpp3 channel activity. *Journal of Neurochemistry*, 103(6):2391–2400.
- Li, Q., Liu, Y., Shen, P. Y., Dai, X. Q., Wang, S., Smillie, L. B., Sandford, R., and Chen, X. Z. (2003). Troponin I binds polycystin-L and inhibits its calcium-induced channel activation. *Biochemistry*, 42(24):7618–7625.
- Ma, S., Yu, H., Zhao, Z., Luo, Z., Chen, J., Ni, Y., Jin, R., Ma, L., Wang, P., Zhu, Z., Li, L., Zhong, J., Liu, D., Nilius, B., and Zhu, Z. (2012). Activation of the cold-sensing trpm8 channel triggers ucpl1-dependent thermogenesis and prevents obesity. *Journal of Molecular Cell Biology*, 4(2):88–96.

- Maleki, M., Ghanbarvand, F., Reza Behvarz, M., Ejtemaei, M., and Ghadirkhomi, E. (2014). Comparison of mesenchymal stem cell markers in multiple human adult stem cells. *Int J Stem Cells*, 7(2):118–126.
- Manders, E. M. M., Verbeek, F. J., and Aten, J. A. (1993). Measurement of co-localization of objects in dual-colour confocal images. *Journal of Microscopy*, 169(3):375–382.
- Marion, V., Mockel, A., De Melo, C., Obringer, C., Claussmann, A., Simon, A., Messaddeq, N., Durand, M., Dupuis, L., Loeffler, J. P., King, P., Mutter-Schmidt, C., Petrovsky, N., Stoetzel, C., and Dollfus, H. (2012). BBS-induced ciliary defect enhances adipogenesis, causing paradoxical higher-insulin sensitivity, glucose usage, and decreased inflammatory response. *Cell Metab.*, 16(3):363–377.
- Marion, V., Stoetzel, C., Schlicht, D., Messaddeq, N., Koch, M., Flori, E., Danse, J. M., Mandel, J. L., and Dollfus, H. (2009). Transient ciliogenesis involving Bardet-Biedl syndrome proteins is a fundamental characteristic of adipogenic differentiation. *Proc. Natl. Acad. Sci. U.S.A.*, 106(6):1820–1825.
- McBeath, R., Pirone, D. M., Nelson, C. M., Bhadriraju, K., and Chen, C. S. (2004). Cell shape, cytoskeletal tension, and RhoA regulate stem cell lineage commitment. *Dev. Cell*, 6(4):483–495.
- Mendez-Ferrer, S., Michurina, T. V., Ferraro, F., Mazloom, A. R., Macarthur, B. D., Lira, S. A., Scadden, D. T., Ma’ayan, A., Enikolopov, G. N., and Frenette, P. S. (2010). Mesenchymal and haematopoietic stem cells form a unique bone marrow niche. *Nature*, 466(7308):829–834.
- Ntuk, U. E., Gill, J. M., Mackay, D. F., Sattar, N., and Pell, J. P. (2014). Ethnic-specific obesity cutoffs for diabetes risk: cross-sectional study of 490,288 UK biobank participants. *Diabetes Care*, 37(9):2500–2507.
- Oberkofler, H., Esterbauer, H., Linnemayr, V., Strosberg, A. D., Krempler, F., and Patsch, W. (2002). Peroxisome proliferator-activated receptor (PPAR) gamma coactivator-1 recruitment regulates PPAR subtype specificity. *J. Biol. Chem.*, 277(19):16750–16757.
- Oh, E. C., Vasanth, S., and Katsanis, N. (2015). Metabolic regulation and energy homeostasis through the primary Cilium. *Cell Metab.*, 21(1):21–31.
- Ono, K., Tsukamoto-Yasui, M., Hara-Kimura, Y., Inoue, N., Nogusa, Y., Okabe, Y., Nagashima, K., and Kato, F. (2011). Intragastric administration of capsiate, a transient receptor potential channel agonist, triggers thermogenic sympathetic responses. *J. Appl. Physiol.*, 110(3):789–798.
- Parham, P. and Ohta, T. (1996). Population biology of antigen presentation by MHC class I molecules. *Science*, 272(5258):67–74.
- Peng, R., Yao, X., and Ding, J. (2011). Effect of cell anisotropy on differentiation of stem cells on micropatterned surfaces through the controlled single cell adhesion. *Biomaterials*, 32(32):8048–8057.
- Phua, S. C., Lin, Y.-C., and Inoue, T. (2015). An intelligent nano-antenna: Primary cilium harnesses {TRP} channels to decode polymodal stimuli. *Cell Calcium*, 58(4):415 – 422. Cell Signalling at Membrane Contact Sites.

- Prosser, S. L. and Morrison, C. G. (2015). Centrin2 regulates CP110 removal in primary cilium formation. *J. Cell Biol.*, 208(6):693–701.
- Qiu, N., Cao, L., David, V., Quarles, L. D., and Xiao, Z. (2010). Kif3a deficiency reverses the skeletal abnormalities in Pkd1 deficient mice by restoring the balance between osteogenesis and adipogenesis. *PLoS ONE*, 5(12):e15240.
- Ross, S. E., Hemati, N., Longo, K. A., Bennett, C. N., Lucas, P. C., Erickson, R. L., and MacDougald, O. A. (2000). Inhibition of adipogenesis by Wnt signaling. *Science*, 289(5481):950–953.
- Rossato, M., Granzotto, M., Macchi, V., Porzionato, A., Petrelli, L., Calcagno, A., Vencato, J., Stefani, D. D., Silvestrin, V., Rizzuto, R., Bassetto, F., Caro, R. D., and Vettor, R. (2014). Human white adipocytes express the cold receptor {TRPM8} which activation induces {UCP1} expression, mitochondrial activation and heat production. *Molecular and Cellular Endocrinology*, 383(1&2):137 – 146.
- Santella, L. and Carafoli, E. (1997). Calcium signaling in the cell nucleus. *FASEB J.*, 11(13):1091–1109.
- Satterthwaite, A. B., Burn, T. C., Le Beau, M. M., and Tenen, D. G. (1992). Structure of the gene encoding CD34, a human hematopoietic stem cell antigen. *Genomics*, 12(4):788–794.
- Schulz, T. J. and Tseng, Y.-H. (2013). Brown adipose tissue: development, metabolism and beyond. *Biochemical Journal*, 453(2):167–178.
- Seale, P., Bjork, B., Yang, W., Kajimura, S., Chin, S., Kuang, S., Scime, A., Devarakonda, S., Conroe, H. M., Erdjument-Bromage, H., Tempst, P., Rudnicki, M. A., Beier, D. R., and Spiegelman, B. M. (2008). PRDM16 controls a brown fat/skeletal muscle switch. *Nature*, 454(7207):961–967.
- Sharp, L. Z., Shinoda, K., Ohno, H., Scheel, D. W., Tomoda, E., Ruiz, L., Hu, H., Wang, L., Pavlova, Z., Gilsanz, V., and Kajimura, S. (2012). Human BAT possesses molecular signatures that resemble beige/brite cells. *PLoS ONE*, 7(11):e49452.
- Shepard, A. R., Jacobson, N., and Clark, A. F. (2005). Importance of quantitative PCR primer location for short interfering RNA efficacy determination. *Anal. Biochem.*, 344(2):287–288.
- Shi, H., Halvorsen, Y. D., Ellis, P. N., Wilkison, W. O., and Zemel, M. B. (2000). Role of intracellular calcium in human adipocyte differentiation. *Physiol. Genomics*, 3(2):75–82.
- Shimizu, T., Higuchi, T., Fujii, T., Nilius, B., and Sakai, H. (2011). Bimodal effect of alkalization on the polycystin transient receptor potential channel, PKD2L1. *Pflugers Arch.*, 461(5):507–513.
- Shimizu, T., Janssens, A., Voets, T., and Nilius, B. (2009). Regulation of the murine TRPP3 channel by voltage, pH, and changes in cell volume. *Pflugers Arch.*, 457(4):795–807.

- Shintaku, K., Uchida, K., Suzuki, Y., Zhou, Y., Fushiki, T., Watanabe, T., Yazawa, S., and Tominaga, M. (2012). Activation of transient receptor potential A1 by a non-pungent capsaicin-like compound, capsiate. *Br. J. Pharmacol.*, 165(5):1476–1486.
- Siiteri, P. K. (1987). Adipose tissue as a source of hormones. *Am. J. Clin. Nutr.*, 45(1 Suppl):277–282.
- Spinsanti, G., Zannolli, R., Panti, C., Ceccarelli, I., Marsili, L., Bachiocco, V., Frati, F., and Aloisi, A. (2008). Quantitative real-time pcr detection of trpv1-4 gene expression in human leukocytes from healthy and hyposensitive subjects. *Molecular Pain*, 4(1):51.
- Sukumar, P., Sedo, A., Li, J., Wilson, L. A., O'Regan, D., Lippiat, J. D., Porter, K. E., Kearney, M. T., Ainscough, J. F., and Beech, D. J. (2012). Constitutively active TRPC channels of adipocytes confer a mechanism for sensing dietary fatty acids and regulating adiponectin. *Circ. Res.*, 111(2):191–200.
- Tedder, T. F. and Isaacs, C. M. (1989). Isolation of cDNAs encoding the CD19 antigen of human and mouse B lymphocytes. A new member of the immunoglobulin superfamily. *J. Immunol.*, 143(2):712–717.
- Tripodskiadis, F., Karayannis, G., Giamouzis, G., Skoularigis, J., Louridas, G., and Butler, J. (2009). The sympathetic nervous system in heart failure physiology, pathophysiology, and clinical implications. *J. Am. Coll. Cardiol.*, 54(19):1747–1762.
- Tsukamoto, H. (2014). [Immune regulation via the generation of extracellular adenosine by CD73]. *Seikagaku*, 86(6):766–769.
- Virtanen, K. A., Lidell, M. E., Orava, J., Heglind, M., Westergren, R., Niemi, T., Taittonen, M., Laine, J., Savisto, N.-J., Enerbäck, S., and Nuutila, P. (2009). Functional brown adipose tissue in healthy adults. *New England Journal of Medicine*, 360(15):1518–1525. PMID: 19357407.
- Wang, H., Zhang, Y., Yehuda-Shnaidman, E., Medvedev, A. V., Kumar, N., Daniel, K. W., Robidoux, J., Czech, M. P., Mangelsdorf, D. J., and Collins, S. (2008). Liver X receptor alpha is a transcriptional repressor of the uncoupling protein 1 gene and the brown fat phenotype. *Mol. Cell. Biol.*, 28(7):2187–2200.
- WHO (2012). The top 10 causes of death.
- Wiesmann, A., Buhning, H. J., Mentrup, C., and Wiesmann, H. P. (2006). Decreased CD90 expression in human mesenchymal stem cells by applying mechanical stimulation. *Head Face Med*, 2:8.
- Winnicka, B., O'Connor, C., Schacke, W., Vernier, K., Grant, C. L., Fenteany, F. H., Pereira, F. E., Liang, B., Kaur, A., Zhao, R., Montrose, D. C., Rosenberg, D. W., Aguila, H. L., and Shapiro, L. H. (2010). CD13 is dispensable for normal hematopoiesis and myeloid cell functions in the mouse. *J. Leukoc. Biol.*, 88(2):347–359.
- Wu, Z., Puigserver, P., and Spiegelman, B. M. (1999). Transcriptional activation of adipogenesis. *Current Opinion in Cell Biology*, 11(6):689 – 694.

- Xue, R., Lynes, M. D., Dreyfuss, J. M., Shamsi, F., Schulz, T. J., Zhang, H., Huang, T. L., Townsend, K. L., Li, Y., Takahashi, H., Weiner, L. S., White, A. P., Lynes, M. S., Rubin, L. L., Goodyear, L. J., Cypess, A. M., and Tseng, Y. H. (2015). Clonal analyses and gene profiling identify genetic biomarkers of the thermogenic potential of human brown and white preadipocytes. *Nat. Med.*, 21(7):760–768.
- Yang, J., Wang, Q., Zheng, W., Tuli, J., Li, Q., Wu, Y., Hussein, S., Dai, X. Q., Shafiei, S., Li, X. G., Shen, P. Y., Tu, J. C., and Chen, X. Z. (2012). Receptor for activated C kinase 1 (RACK1) inhibits function of transient receptor potential (TRP)-type channel Pkd2L1 through physical interaction. *J. Biol. Chem.*, 287(9):6551–6561.
- Ye, J., Coulouris, G., Zaretskaya, I., Cutcutache, I., Rozen, S., and Madden, T. L. (2012a). Primer-BLAST: a tool to design target-specific primers for polymerase chain reaction. *BMC Bioinformatics*, 13:134.
- Ye, L., Kleiner, S., Wu, J., Sah, R., Gupta, R. K., Banks, A. S., Cohen, P., Khandekar, M. J., Bostrom, P., Mepani, R. J., Laznik, D., Kamenecka, T. M., Song, X., Liedtke, W., Mootha, V. K., Puigserver, P., Griffin, P. R., Clapham, D. E., and Spiegelman, B. M. (2012b). TRPV4 is a regulator of adipose oxidative metabolism, inflammation, and energy homeostasis. *Cell*, 151(1):96–110.
- Zheng, W., Hussein, S., Yang, J., Huang, J., Zhang, F., Hernandez-Anzaldo, S., Fernandez-Patron, C., Cao, Y., Zeng, H., Tang, J., and Chen, X. Z. (2015). A novel PKD2L1 C-terminal domain critical for trimerization and channel function. *Sci Rep*, 5:9460.
- Zhou, J. (2009). Polycystins and primary cilia: Primers for cell cycle progression. *Annual Review of Physiology*, 71(1):83–113. PMID: 19572811.
- Ziegler-Heitbrock, H. W. and Ulevitch, R. J. (1993). CD14: cell surface receptor and differentiation marker. *Immunol. Today*, 14(3):121–125.